Incoherent J/ψ production at large $|t|$ identifies the onset of saturation at the LHC

J. Cepila[a], J. G. Contreras[a], M. Matas[a], A. Ridzikova[a]

[a] *Faculty of Nuclear Sciences and Physical Engineering, Czech Technical University in Prague, Czech Republic*

International Workshop on Deep Inelastic Scattering and Related Subjects

10.04.2024

Alexandra Ridziková

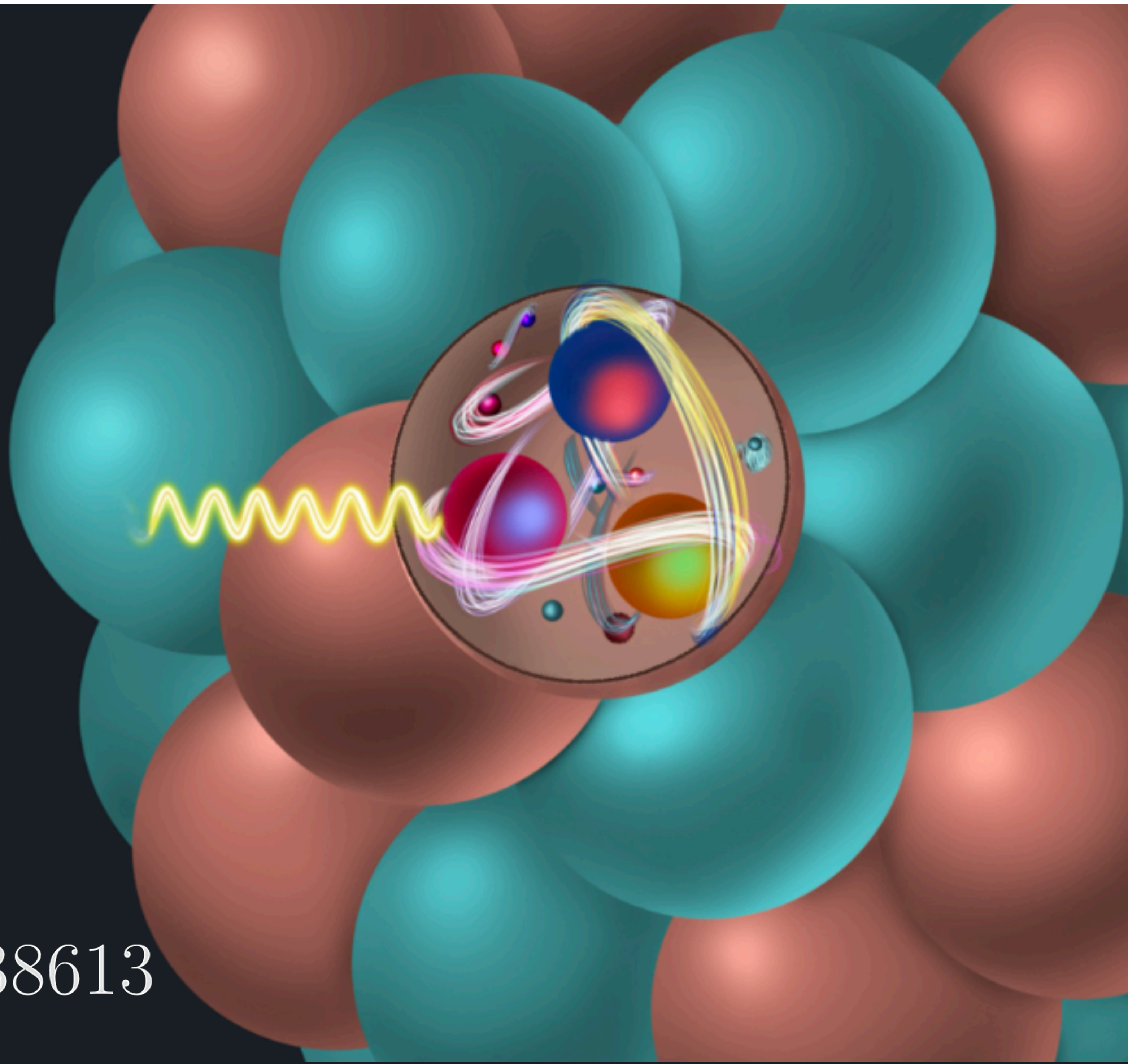

The work is based on
arXiv:2312.11320 [hep-ph] Phys. Lett. B 852 (2024) 138613

MOTIVATION

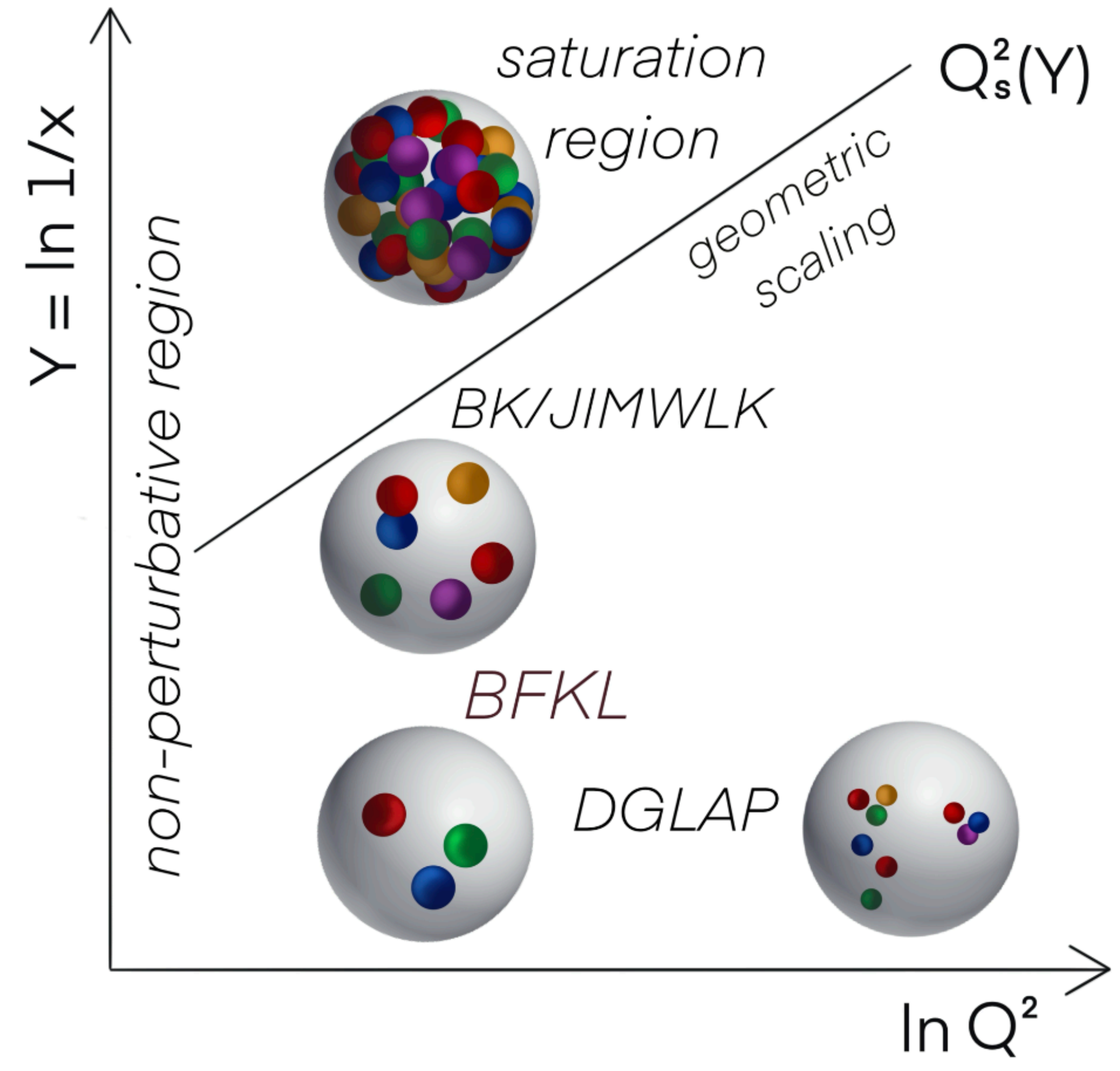

saturation
region
$Q_s^2(Y)$
geometric
scaling
BK/JIMWLK
BFKL
DGLAP
non-perturbative region
Y = ln 1/x
ln Q²

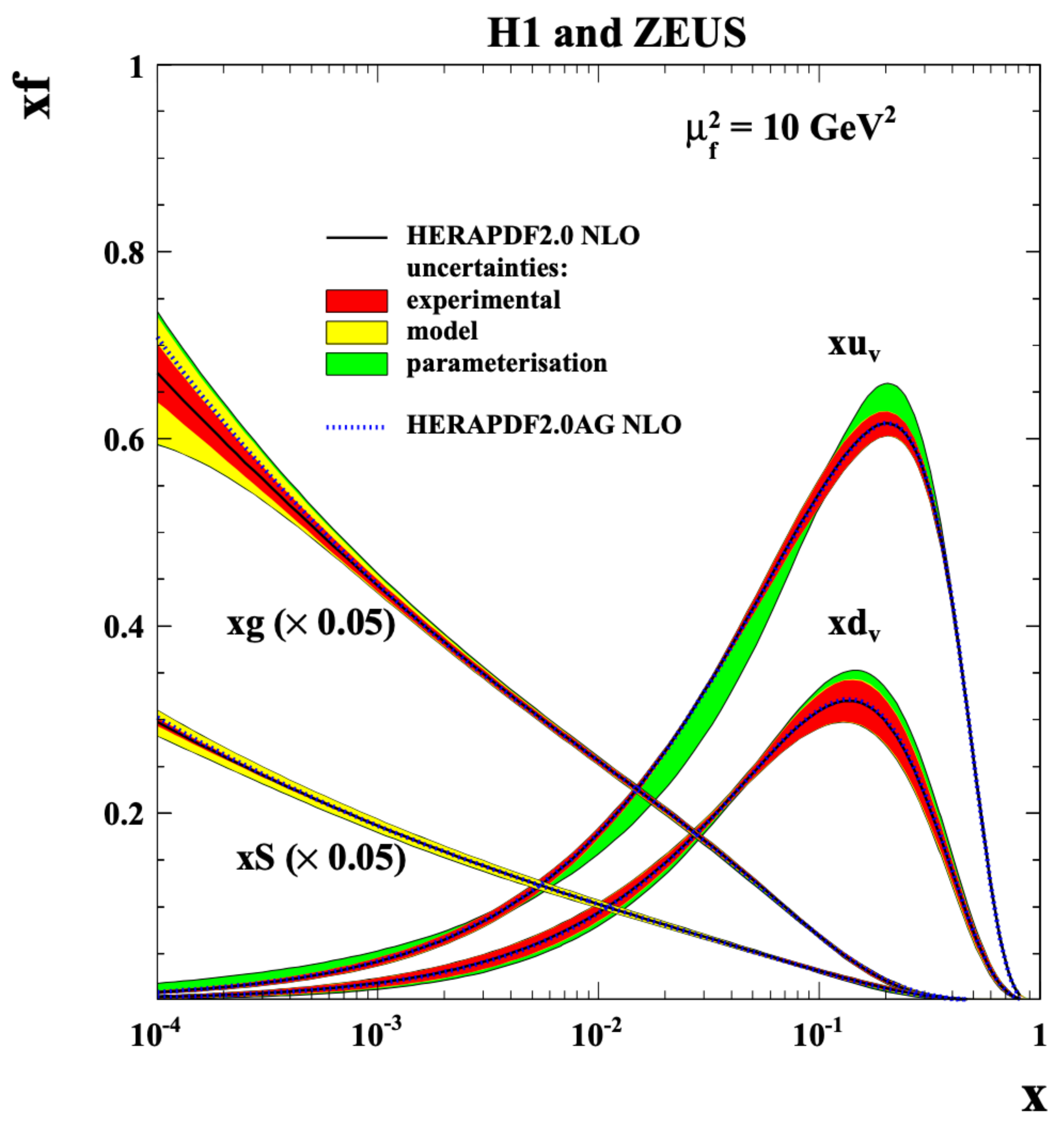

H1 and ZEUS
xf
μ_f^2 = 10 GeV²
HERAPDF2.0 NLO
uncertainties:
experimental
model
parameterisation
HERAPDF2.0AG NLO
xu_v
xd_v
xg (× 0.05)
xS (× 0.05)
x

MOTIVATION

- Due to the high density in small-x region, the radiated gluons overlap each other and start interacting: ONSET OF SATURATION
  - The DIFFRACTIVE VECTOR MESON PRODUCTION serve as valuable tool for probing saturation effects due to its sensitivity to the gluon distribution within hadrons

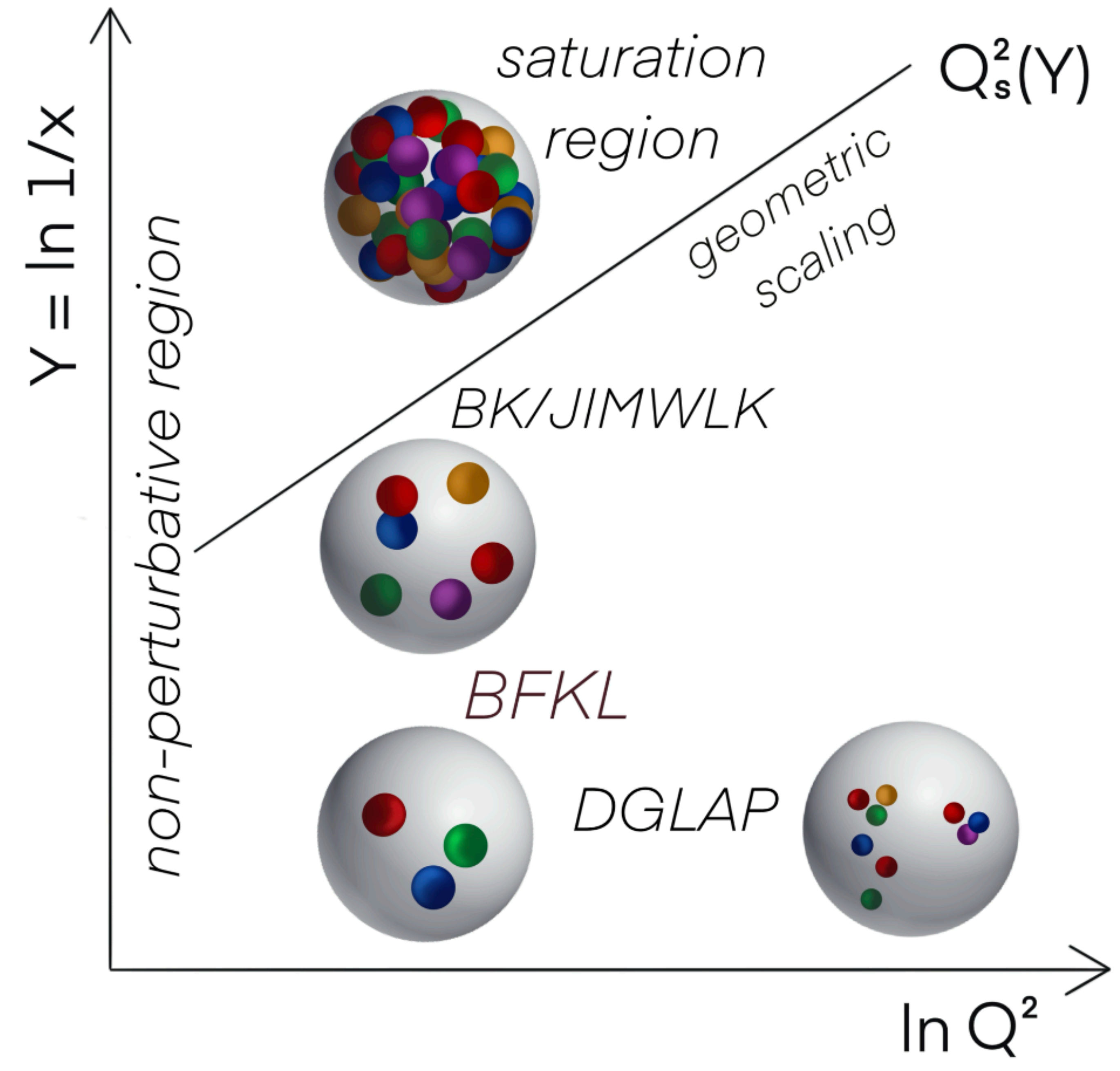

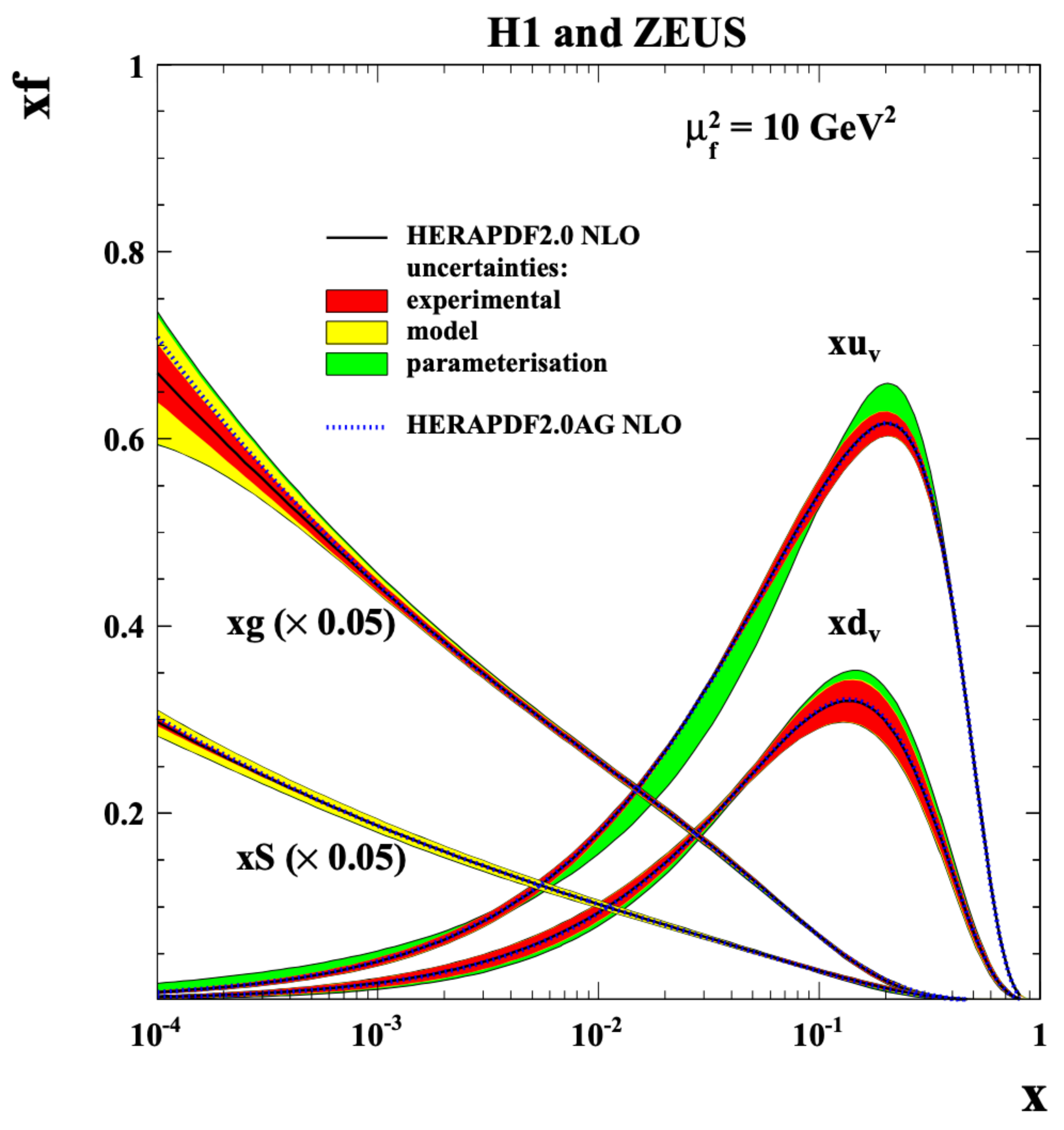

VECTOR MESON PRODUCTION

COHERENT

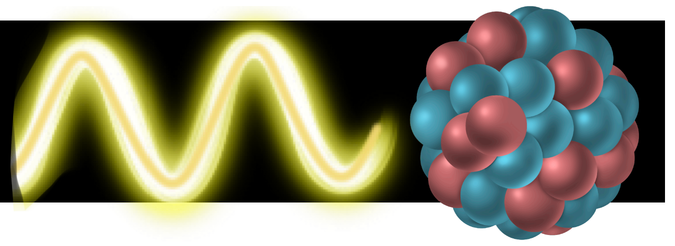

$$\left.\frac{\mathrm{d}\sigma^{\gamma^* \mathrm{H}\to \mathrm{VH}}}{\mathrm{d}|t|}\right|_{\mathrm{T,L}} = \frac{\left(R_g^{\mathrm{T,L}}\right)^2}{16\pi} |\langle \mathcal{A}_{\mathrm{T,L}}\rangle|^2$$

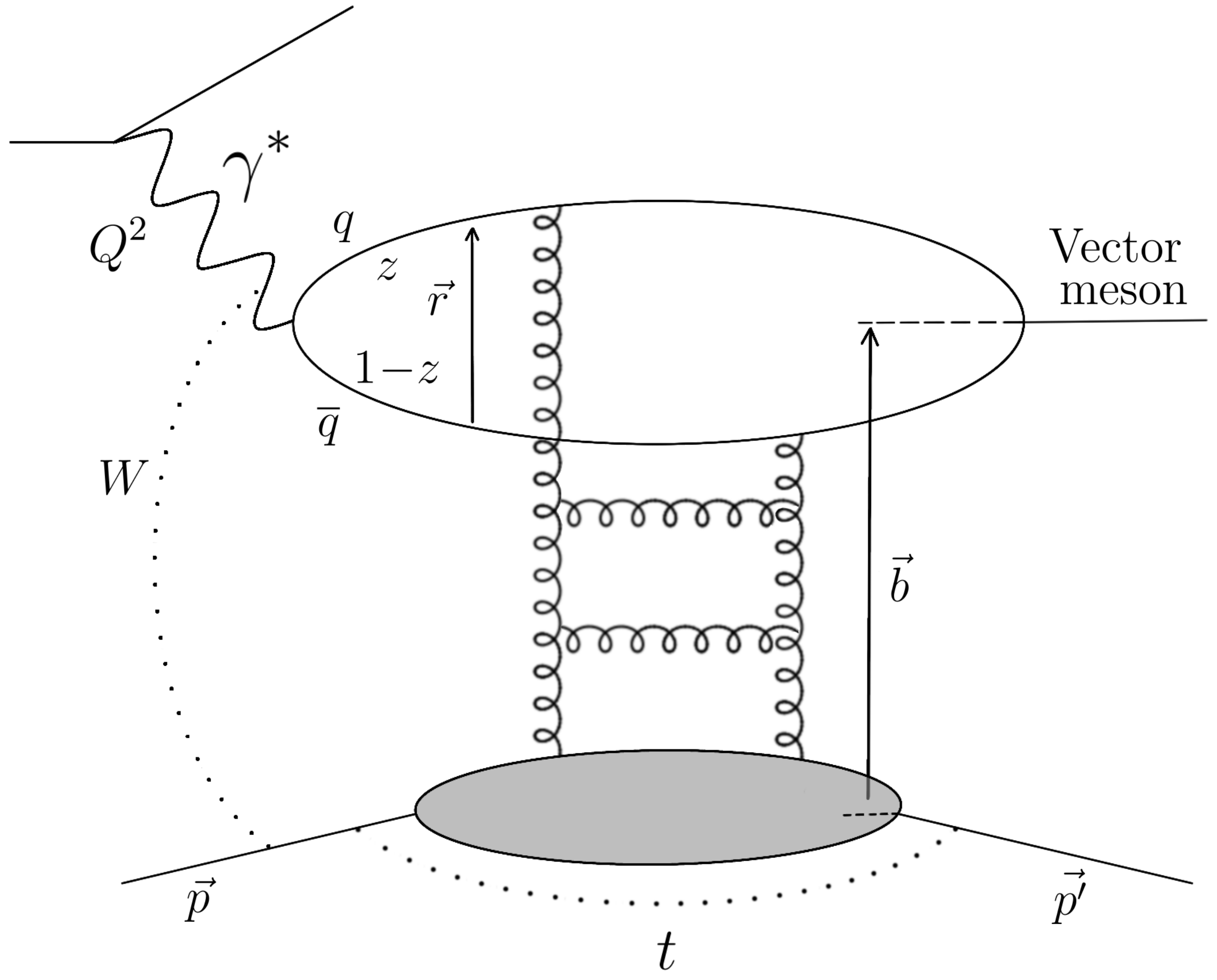

$$x = \frac{Q^2 + M^2}{Q^2 + W^2}$$

- Bjorken-x of the produced meson

$$W$$

- the centre-of-mass energy of the photon-target system

INCOHERENT

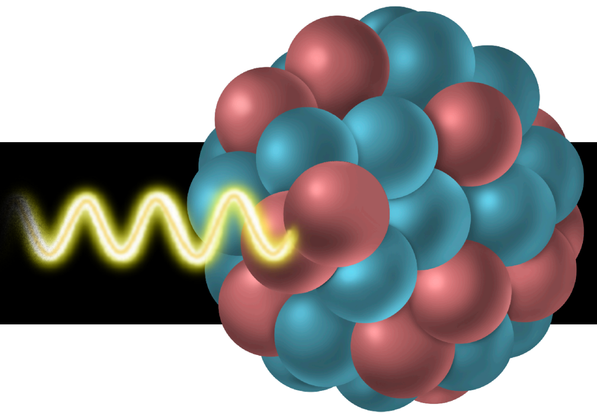

DISSOCIATIVE

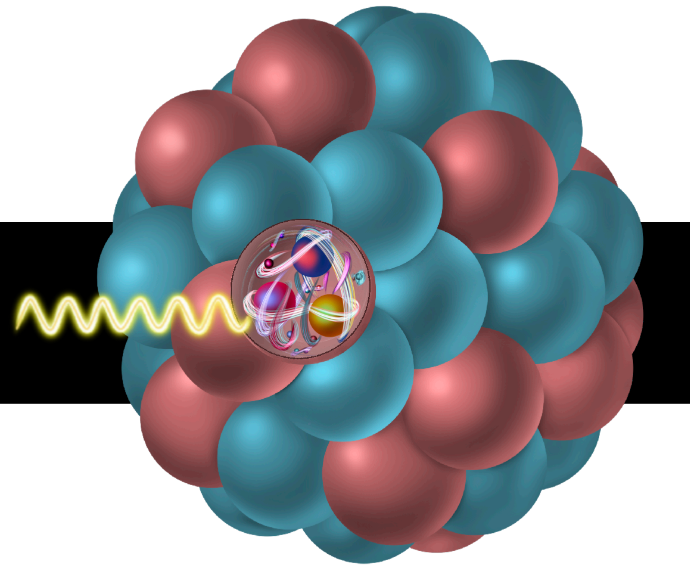

$$\left.\frac{\mathrm{d}\sigma^{\gamma^* p\to \mathrm{V}Y}}{\mathrm{d}|t|}\right|_{\mathrm{T,L}} = \frac{\left(R_g^{T,L}\right)^2}{16\pi} \left(\langle|\mathcal{A}_{\mathrm{T,L}}|^2\rangle - |\langle \mathcal{A}_{\mathrm{T,L}}\rangle|^2\right)$$

$$t = (p' - p)^2 = -\Delta^2$$

- the square of the momentum transferred in the interaction

- The scattering amplitude of the process is given by the convolution of photon and vector meson wave functions $|\Psi_{\rm V}^{*}\Psi_{\gamma^{*}}|_{\rm T,L}$ and the differential dipole cross section $\frac{{\rm d}\sigma^{\rm dip}}{{\rm d}\vec{b}}$

$$\mathcal{A}_{\rm T,L}(x,Q^2,\vec{\Delta}) = i\int {\rm d}\vec{r}\int_0^1 \frac{{\rm d}z}{4\pi}\int {\rm d}\vec{b}|\Psi_{\rm V}^{*}\Psi_{\gamma^{*}}|_{\rm T,L}\exp\left[-i\left(\vec{b}-(\frac{1}{2}-z)\vec{r}\right)\vec{\Delta}\right]\frac{{\rm d}\sigma^{\rm dip}}{{\rm d}\vec{b}}$$

- The targets that we consider are proton *(p)* and lead *(Pb)*

- The scattering amplitude of the process is given by the convolution of photon and vector meson wave functions $|\Psi_{\mathrm{V}}^{*}\Psi_{\gamma^*}|_{\mathrm{T,L}}$ and the differential dipole cross section $\frac{\mathrm{d}\sigma^{\mathrm{dip}}}{\mathrm{d}\vec{b}}$

$$\mathcal{A}_{\mathrm{T,L}}(x,Q^2,\vec{\Delta}) = i\int \mathrm{d}\vec{r}\int_0^1 \frac{\mathrm{d}z}{4\pi}\int \mathrm{d}\vec{b}|\Psi_{\mathrm{V}}^{*}\Psi_{\gamma^*}|_{\mathrm{T,L}} \exp\left[-i\left(\vec{b}-(\frac{1}{2}-z)\vec{r}\right)\vec{\Delta}\right]\frac{\mathrm{d}\sigma^{\mathrm{dip}}}{\mathrm{d}\vec{b}}$$

- The targets that we consider are proton *(p)* and lead *(Pb)*

PROTON

$$\frac{\mathrm{d}\sigma_{\mathrm{p}}^{\mathrm{dip}}}{\mathrm{d}\vec{b}} = \sigma_0 N(x,r)T_{\mathrm{p}}(\vec{b})$$

$$T_{\mathrm{p}}(\vec{b}) = \frac{1}{N_{\mathrm{hs}}}\sum_{i=1}^{N_{\mathrm{hs}}} T_{\mathrm{hs}}\left(\vec{b}-\vec{b}_i\right)$$

$$T_{\mathrm{hs}}(\vec{b}-\vec{b}_i) = \frac{1}{2\pi B_{\mathrm{hs}}}\exp\left(-\frac{\left(\vec{b}-\vec{b}_i\right)^2}{2B_{\mathrm{hs}}}\right)$$

arXiv:1608.07559 [hep-ph]

- The scattering amplitude of the process is given by the convolution of photon and vector meson wave functions $|\Psi_{\mathrm{V}}^{*}\Psi_{\gamma^{*}}|_{\mathrm{T,L}}$ and the differential dipole cross section $\frac{\mathrm{d}\sigma^{\mathrm{dip}}}{\mathrm{d}\vec{b}}$

$$\mathcal{A}_{\mathrm{T,L}}(x, Q^2, \vec{\Delta}) = i \int \mathrm{d}\vec{r} \int_0^1 \frac{\mathrm{d}z}{4\pi} \int \mathrm{d}\vec{b} |\Psi_{\mathrm{V}}^{*}\Psi_{\gamma^{*}}|_{\mathrm{T,L}} \exp\left[-i\left(\vec{b} - (\frac{1}{2} - z)\vec{r}\right)\vec{\Delta}\right] \frac{\mathrm{d}\sigma^{\mathrm{dip}}}{\mathrm{d}\vec{b}}$$

- The targets that we consider are proton *(p)* and lead *(Pb)*

PROTON

$$\frac{\mathrm{d}\sigma_{\mathrm{p}}^{\mathrm{dip}}}{\mathrm{d}\vec{b}} = \sigma_0 N(x, r) T_{\mathrm{p}}(\vec{b})$$

$$T_{\mathrm{p}}(\vec{b}) = \frac{1}{N_{\mathrm{hs}}} \sum_{i=1}^{N_{\mathrm{hs}}} T_{\mathrm{hs}}\left(\vec{b} - \vec{b}_i\right)$$

$$T_{\mathrm{hs}}(\vec{b} - \vec{b}_i) = \frac{1}{2\pi B_{\mathrm{hs}}} \exp\left(-\frac{\left(\vec{b} - \vec{b}_i\right)^2}{2B_{\mathrm{hs}}}\right)$$

arXiv:1608.07559 [hep-ph]

GBW MODEL

$$N(x, r) = \left[1 - \exp\left(-\frac{r^2 Q_s^2(x)}{4}\right)\right]$$

$$\langle N_{hs}(x)\rangle = p_0 x^{p_1}(1 + p_2\sqrt{x})$$

- The scattering amplitude of the process is given by the convolution of photon and vector meson wave functions $|\Psi_V^* \Psi_{\gamma^*}|_{T,L}$ and the differential dipole cross section $\frac{\mathrm{d}\sigma^{\mathrm{dip}}}{\mathrm{d}\vec{b}}$

$$\mathcal{A}_{T,L}(x, Q^2, \vec{\Delta}) = i \int \mathrm{d}\vec{r} \int_0^1 \frac{\mathrm{d}z}{4\pi} \int \mathrm{d}\vec{b} |\Psi_V^* \Psi_{\gamma^*}|_{T,L} \exp\left[-i\left(\vec{b} - (\frac{1}{2} - z)\vec{r}\right)\vec{\Delta}\right] \frac{\mathrm{d}\sigma^{\mathrm{dip}}}{\mathrm{d}\vec{b}}$$

- The targets that we consider are proton *(p)* and lead *(Pb)*

ENERGY-DEPENDENT HOT–SPOT MODEL

PROTON

$$\frac{\mathrm{d}\sigma_p^{\mathrm{dip}}}{\mathrm{d}\vec{b}} = \sigma_0 N(x, r) T_p(\vec{b})$$

GBW MODEL

$$N(x, r) = \left[1 - \exp\left(-\frac{r^2 Q_s^2(x)}{4}\right)\right]$$

$$T_p(\vec{b}) = \frac{1}{N_{hs}} \sum_{i=1}^{N_{hs}} T_{hs}\left(\vec{b} - \vec{b}_i\right)$$

$$\langle N_{hs}(x) \rangle = p_0 x^{p_1}(1 + p_2\sqrt{x})$$

NUMBER OF HOT SPOTS

$$T_{hs}(\vec{b} - \vec{b}_i) = \frac{1}{2\pi B_{hs}} \exp\left(-\frac{\left(\vec{b} - \vec{b}_i\right)^2}{2B_{hs}}\right)$$

arXiv:1608.07559 [hep-ph]

ENERGY-DEPENDENT HOT–SPOT MODEL

PROTON

$$\frac{d\sigma_p^{dip}}{d\vec{b}} = \sigma_0 N(x,r) T_p(\vec{b})$$

$$T_p(\vec{b}) = \frac{1}{N_{hs}} \sum_{i=1}^{N_{hs}} T_{hs}\left(\vec{b} - \vec{b}_i\right)$$

$$T_{hs}(\vec{b} - \vec{b}_i) = \frac{1}{2\pi B_{hs}} \exp\left(-\frac{\left(\vec{b} - \vec{b}_i\right)^2}{2B_{hs}}\right)$$

arXiv:1608.07559 [hep-ph]

$$N(x,r) = \left[1 - \exp\left(-\frac{r^2 Q_s^2(x)}{4}\right)\right]$$

$$\langle N_{hs}(x)\rangle = p_0 x^{p_1}(1 + p_2\sqrt{x})$$

THE KEY FEATURE OF OUR MODEL IS THE EVOLUTION OF THE NUMBER OF HOT SPOTS WITH ENERGY IN ORDER TO REFLECT THE RAISE OF THE GLUON DISTRIBUTION, AS BJORKEN-X DECREASES

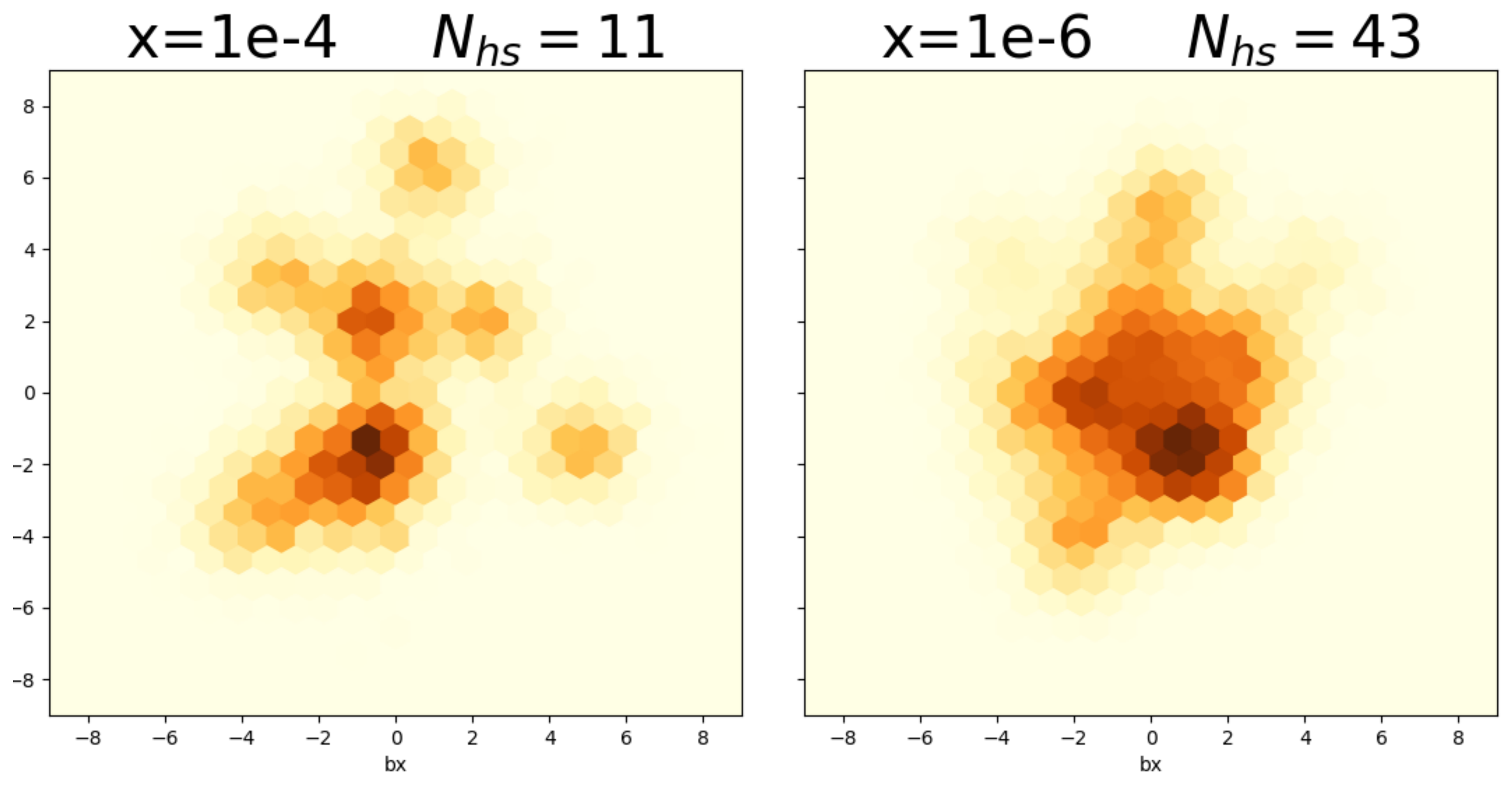

ENERGY-DEPENDENT HOT–SPOT MODEL

PROTON

$$\frac{d\sigma_p^{dip}}{d\vec{b}} = \sigma_0 N(x,r) T_p(\vec{b})$$

$$T_p(\vec{b}) = \frac{1}{N_{hs}} \sum_{i=1}^{N_{hs}} T_{hs}\left(\vec{b} - \vec{b}_i\right)$$

$$T_{hs}(\vec{b} - \vec{b}_i) = \frac{1}{2\pi B_{hs}} \exp\left(-\frac{\left(\vec{b} - \vec{b}_i\right)^2}{2B_{hs}}\right)$$

arXiv:1608.07559 [hep-ph]

$$N(x,r) = \left[1 - \exp\left(-\frac{r^2 Q_s^2(x)}{4}\right)\right]$$

$$\langle N_{hs}(x) \rangle = p_0 x^{p_1} (1 + p_2 \sqrt{x})$$

THE KEY FEATURE OF OUR MODEL IS THE EVOLUTION OF THE NUMBER OF HOT SPOTS WITH ENERGY IN ORDER TO REFLECT THE RAISE OF THE GLUON DISTRIBUTION, AS BJORKEN-X DECREASES

- The position of hotspot, $\vec{b}_i$ is randomly sampled from *2D* Gaussian distribution of width B_p and centred at *(0,0)*
- B_p and B_{hs} represent one-half of the averaged squared radius of the proton and of the hot spot, respectively
- $\sigma_0 = 4\pi B_p$ is twice the transverse area of the proton

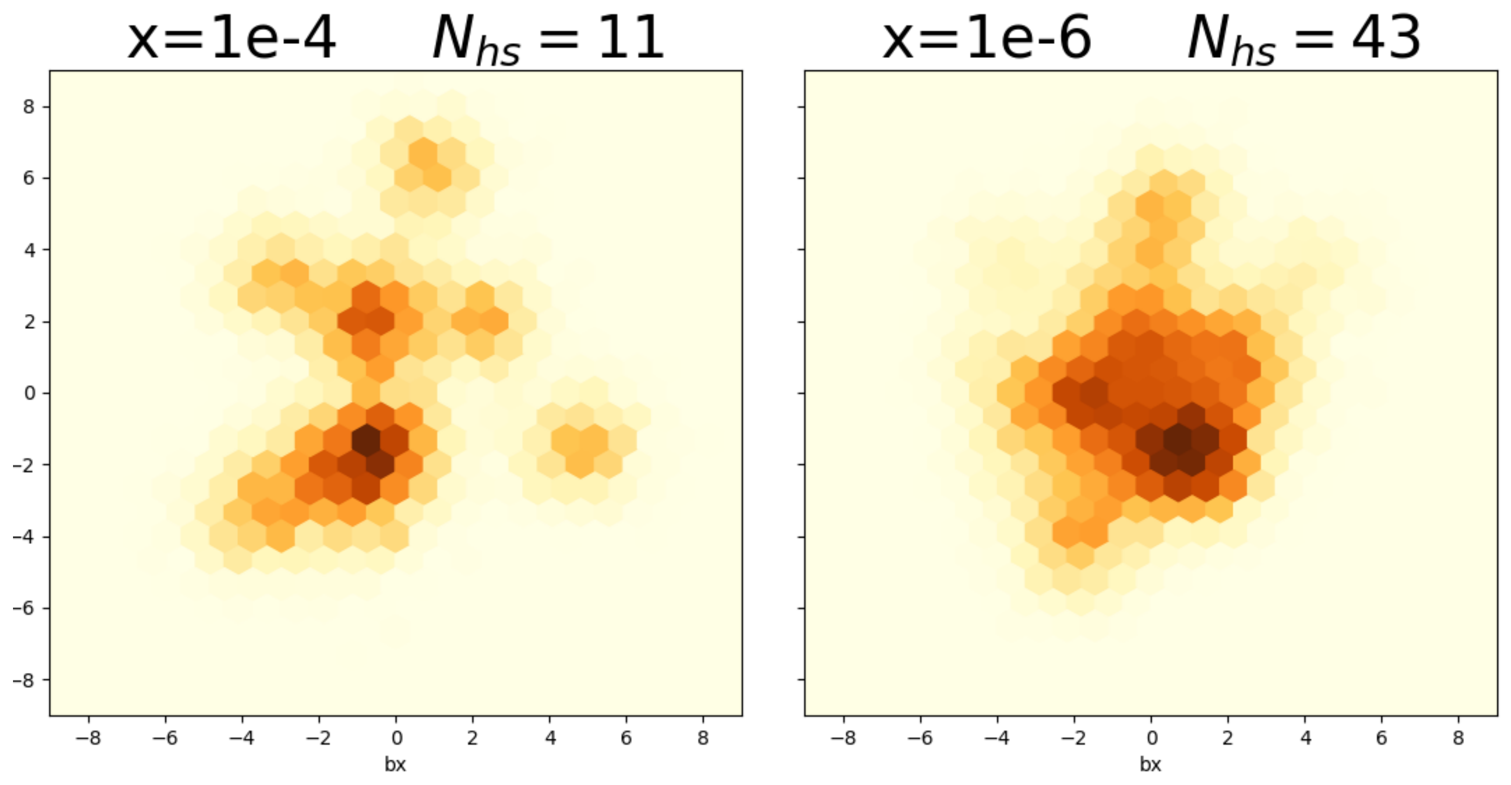

ENERGY-DEPENDENT HOT–SPOT MODEL

PROTON

$$\frac{\mathrm{d}\sigma_{\mathrm{p}}^{\mathrm{dip}}}{\mathrm{d}\vec{b}} = \sigma_0 N(x,r) T_{\mathrm{p}}(\vec{b})$$

$$T_{\mathrm{p}}(\vec{b}) = \frac{1}{N_{\mathrm{hs}}} \sum_{i=1}^{N_{\mathrm{hs}}} T_{\mathrm{hs}}\left(\vec{b}-\vec{b}_i\right)$$

$$T_{\mathrm{hs}}(\vec{b}-\vec{b}_i) = \frac{1}{2\pi B_{\mathrm{hs}}} \exp\left(-\frac{\left(\vec{b}-\vec{b}_i\right)^2}{2B_{\mathrm{hs}}}\right)$$

arXiv:1608.07559 [hep-ph]

$$N(x,r) = \left[1 - \exp\left(-\frac{r^2 Q_s^2(x)}{4}\right)\right]$$

$$\langle N_{hs}(x)\rangle = p_0 x^{p_1}(1 + p_2\sqrt{x})$$

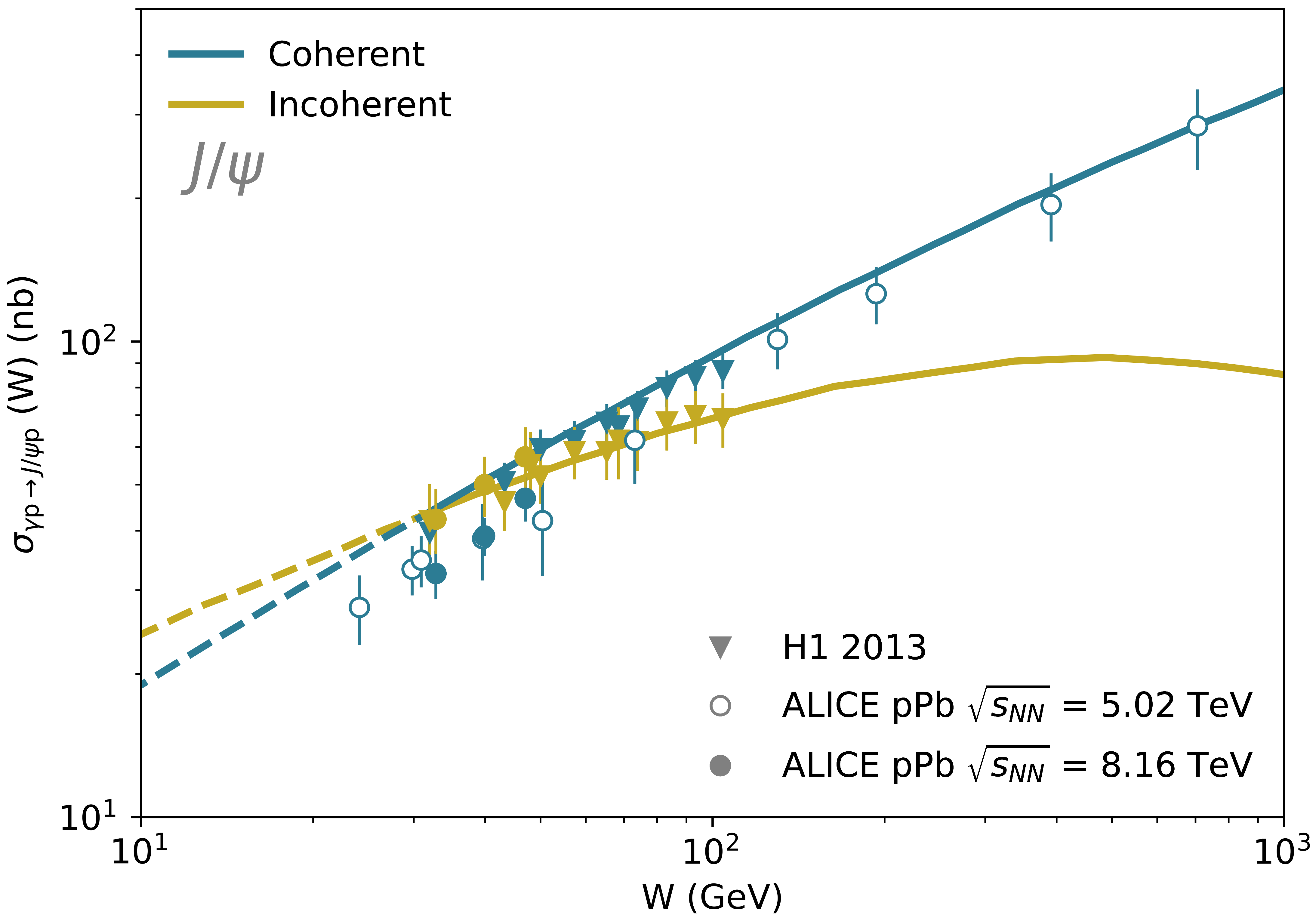

Diffractive photo-production of J/ψ off protons for the coherent (blue) and incoherent (gold) processes.

ENERGY-DEPENDENT HOT–SPOT MODEL

PROTON

$$\frac{\mathrm{d}\sigma_{\mathrm{p}}^{\mathrm{dip}}}{\mathrm{d}\vec{b}} = \sigma_0 N(x,r) T_{\mathrm{p}}(\vec{b})$$

$$T_{\mathrm{p}}(\vec{b}) = \frac{1}{N_{\mathrm{hs}}} \sum_{i=1}^{N_{\mathrm{hs}}} T_{\mathrm{hs}}\left(\vec{b} - \vec{b}_i\right)$$

$$T_{\mathrm{hs}}(\vec{b} - \vec{b}_i) = \frac{1}{2\pi B_{\mathrm{hs}}} \exp\left(-\frac{\left(\vec{b} - \vec{b}_i\right)^2}{2B_{\mathrm{hs}}}\right)$$

arXiv:1608.07559 [hep-ph]

$$N(x,r) = \left[1 - \exp\left(-\frac{r^2 Q_s^2(x)}{4}\right)\right]$$

$$\langle N_{hs}(x) \rangle = p_0 x^{p_1}(1 + p_2\sqrt{x})$$

~500 GeV THE CROSS SECTION STARTS TO DECREASE

- the fact that the variance decreases signifies that the configurations start to resemble each other, which marks the onset of saturation

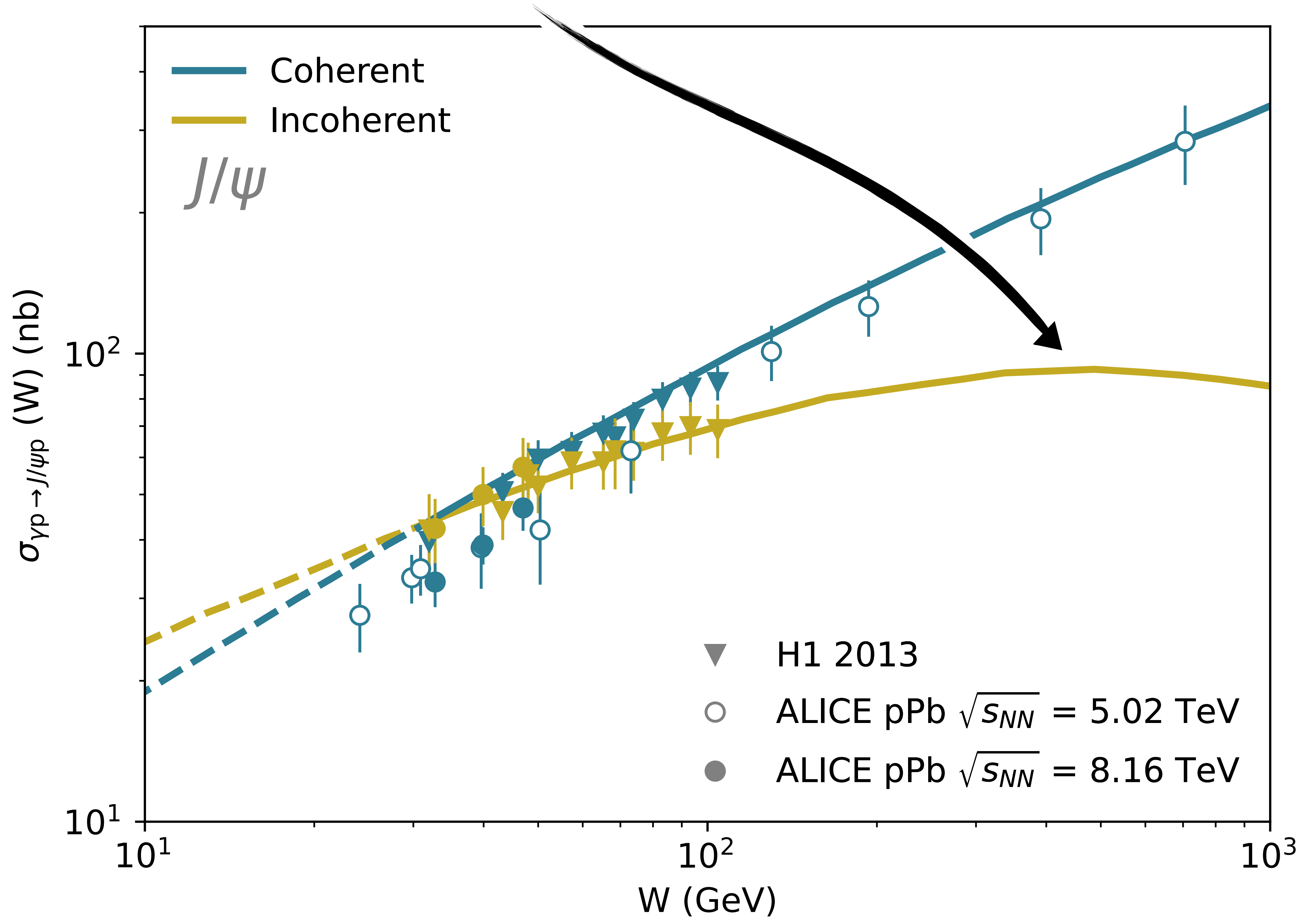

Diffractive photo-production of J/ψ off protons for the coherent (blue) and incoherent (gold) processes.

ENERGY-DEPENDENT HOT–SPOT MODEL

LEAD

$$\frac{d\sigma_{\mathrm{Pb}}^{\mathrm{dip}}}{d\vec{b}} = 2\left[1 - \left(1 - \frac{1}{2A}\sigma_0 N(x,r) T_{\mathrm{Pb}}(\vec{b})\right)^A\right]$$

$$T_{\mathrm{hs}}(\vec{b}-\vec{b}_i) = \frac{1}{2\pi B_{\mathrm{hs}}} \sum_{i=1}^{A=208} \frac{1}{N_{\mathrm{hs}}} \sum_{j=1}^{N_{\mathrm{hs}}} \exp\left(-\frac{\left(\vec{b}-\vec{b}_i-\vec{b}_j\right)^2}{2B_{\mathrm{hs}}}\right)$$

$$N(x,r) = \left[1 - \exp\left(-\frac{r^2 Q_s^2(x)}{4}\right)\right]$$

$$\langle N_{hs}(x)\rangle = p_0 x^{p_1}(1 + p_2\sqrt{x})$$

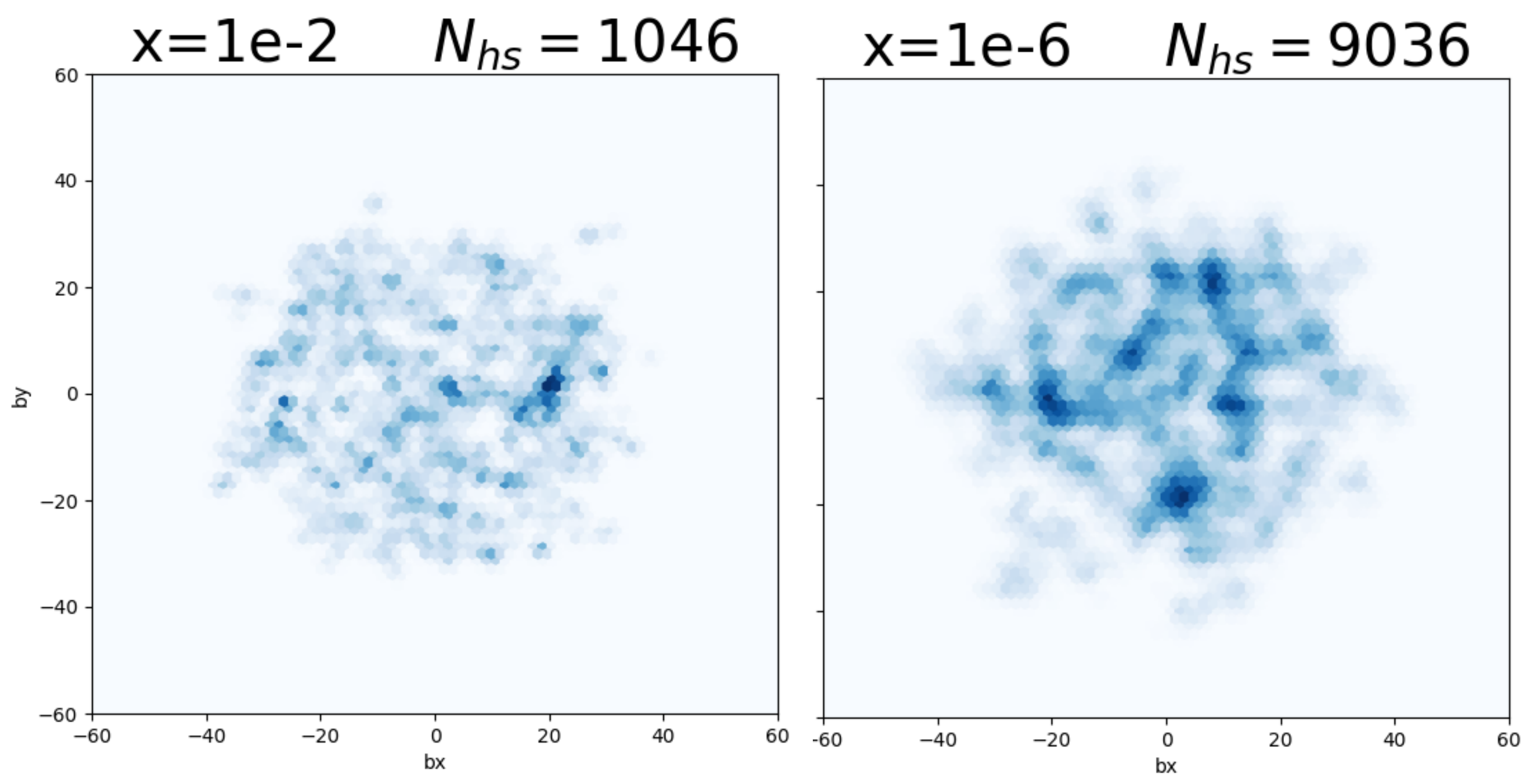

ENERGY-DEPENDENT HOT–SPOT MODEL

LEAD

$$\frac{\mathrm{d}\sigma_{\mathrm{Pb}}^{\mathrm{dip}}}{\mathrm{d}\vec{b}} = 2\left[1-\left(1-\frac{1}{2A}\sigma_0 N(x,r)T_{\mathrm{Pb}}(\vec{b})\right)^{A}\right]$$

NUCLEAR PROFILE

$$T_{\mathrm{hs}}(\vec{b}-\vec{b}_i) = \frac{1}{2\pi B_{\mathrm{hs}}}\sum_{i=1}^{A=208}\frac{1}{N_{\mathrm{hs}}}\sum_{j=1}^{N_{\mathrm{hs}}}\exp\left(-\frac{\left(\vec{b}-\vec{b}_i-\vec{b}_j\right)^2}{2B_{\mathrm{hs}}}\right)$$

- Position of nucleons is chosen randomly from the Woods-Saxon distribution

$$N(x,r) = \left[1-\exp\left(-\frac{r^2 Q_s^2(x)}{4}\right)\right]$$

$$\langle N_{hs}(x)\rangle = p_0 x^{p_1}(1+p_2\sqrt{x})$$

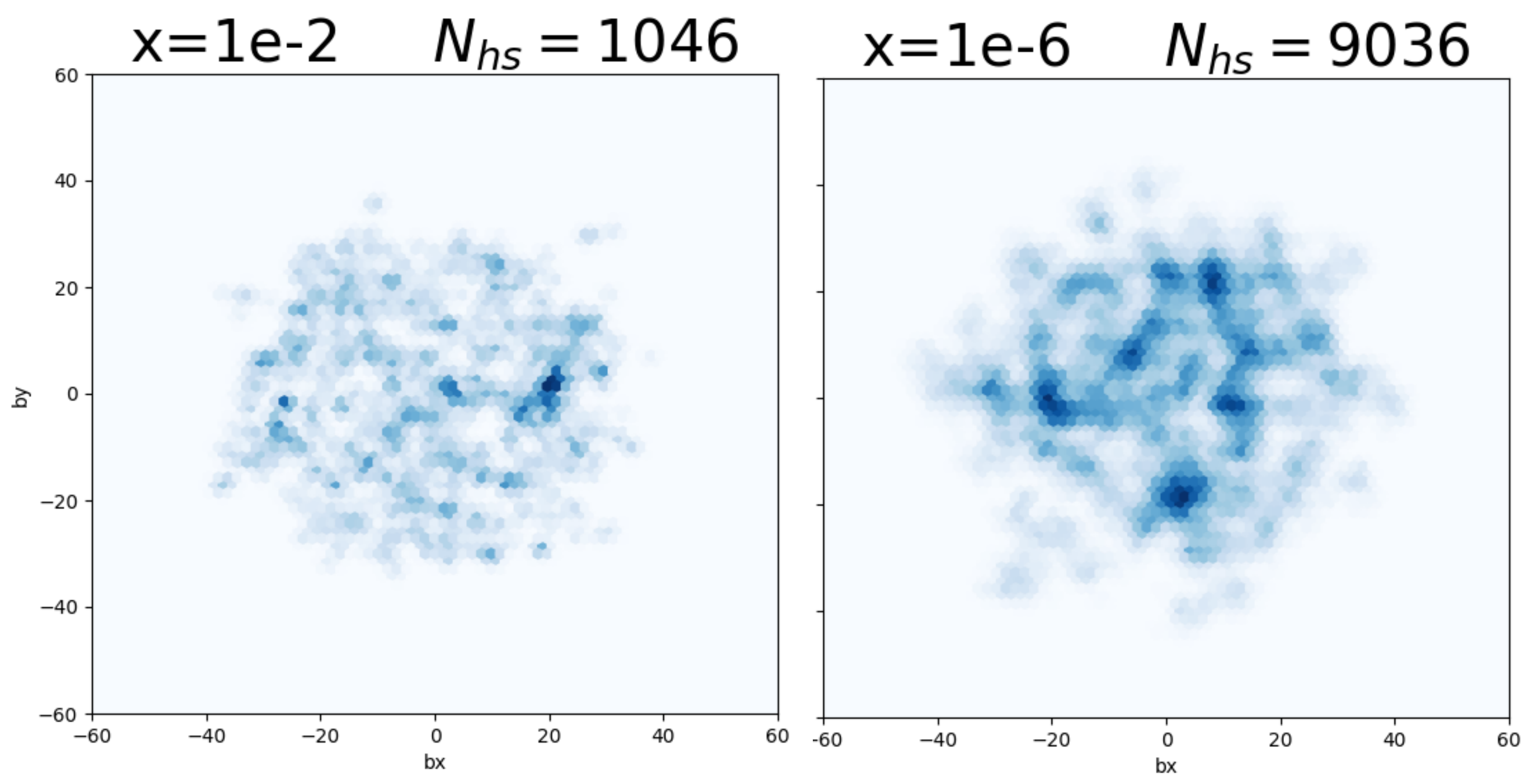

ENERGY-DEPENDENT HOT–SPOT MODEL

LEAD

$$\frac{\mathrm{d}\sigma^{\mathrm{dip}}_{\mathrm{Pb}}}{\mathrm{d}\vec{b}} = 2\left[1-\left(1-\frac{1}{2A}\sigma_0 N(x,r)T_{\mathrm{Pb}}(\vec{b})\right)^A\right]$$

$$T_{\mathrm{hs}}(\vec{b}-\vec{b}_i) = \frac{1}{2\pi B_{\mathrm{hs}}}\sum_{i=1}^{A=208}\frac{1}{N_{\mathrm{hs}}}\sum_{j=1}^{N_{\mathrm{hs}}}\exp\left(-\frac{\left(\vec{b}-\vec{b}_i-\vec{b}_j\right)^2}{2B_{\mathrm{hs}}}\right)$$

- Position of nucleons is chosen randomly from the Woods-Saxon distribution

NUCLEAR PROFILE

COHERENT AND INCOHERENT DIFFRACTIVE PRODUCTION OFF NUCLEAR TARGETS OFFERS THE ADVANTAGE THAT SATURATION SETS IN AT A LOWER ENERGY THAN FOR THE CASE OF PROTON

- It is expected that saturation is mainly linked to the hot-spot degrees of freedom

$$N(x,r) = \left[1-\exp\left(-\frac{r^2Q_s^2(x)}{4}\right)\right]$$

$$\langle N_{hs}(x)\rangle = p_0 x^{p_1}(1+p_2\sqrt{x})$$

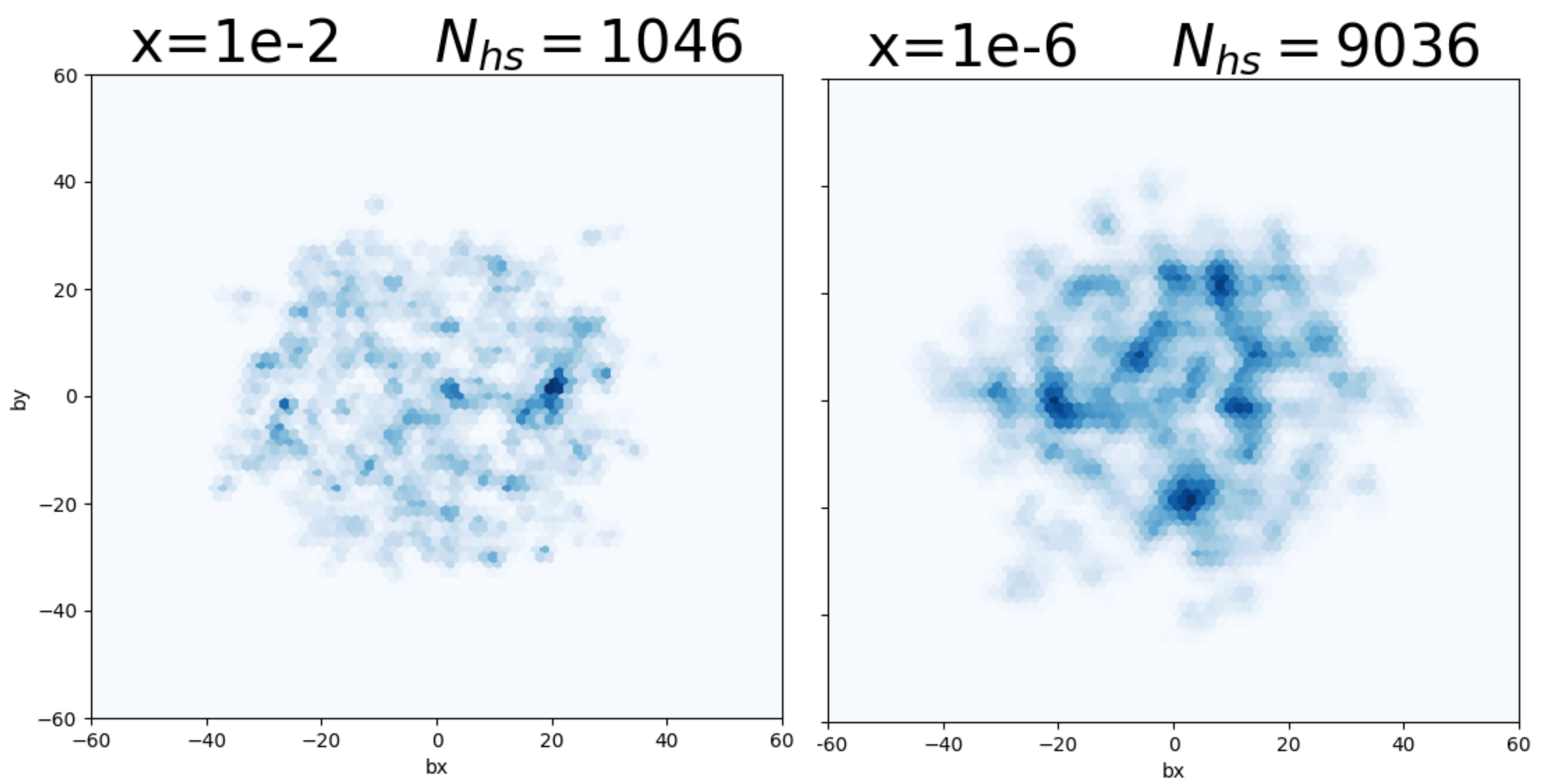

ENERGY-DEPENDENT HOT–SPOT MODEL

LEAD

$$\frac{\mathrm{d}\sigma^{\mathrm{dip}}_{\mathrm{Pb}}}{\mathrm{d}\vec{b}} = 2\left[1-\left(1-\frac{1}{2A}\sigma_0 N(x,r) T_{\mathrm{Pb}}(\vec{b})\right)^A\right]$$

$$T_{\mathrm{hs}}(\vec{b}-\vec{b}_i) = \frac{1}{2\pi B_{\mathrm{hs}}}\sum_{i=1}^{A=208}\frac{1}{N_{\mathrm{hs}}}\sum_{j=1}^{N_{\mathrm{hs}}}\exp\left(-\frac{\left(\vec{b}-\vec{b}_i-\vec{b}_j\right)^2}{2B_{\mathrm{hs}}}\right)$$

$$N(x,r) = \left[1-\exp\left(-\frac{r^2 Q_s^2(x)}{4}\right)\right]$$

$$\langle N_{hs}(x)\rangle = p_0 x^{p_1}(1+p_2\sqrt{x})$$

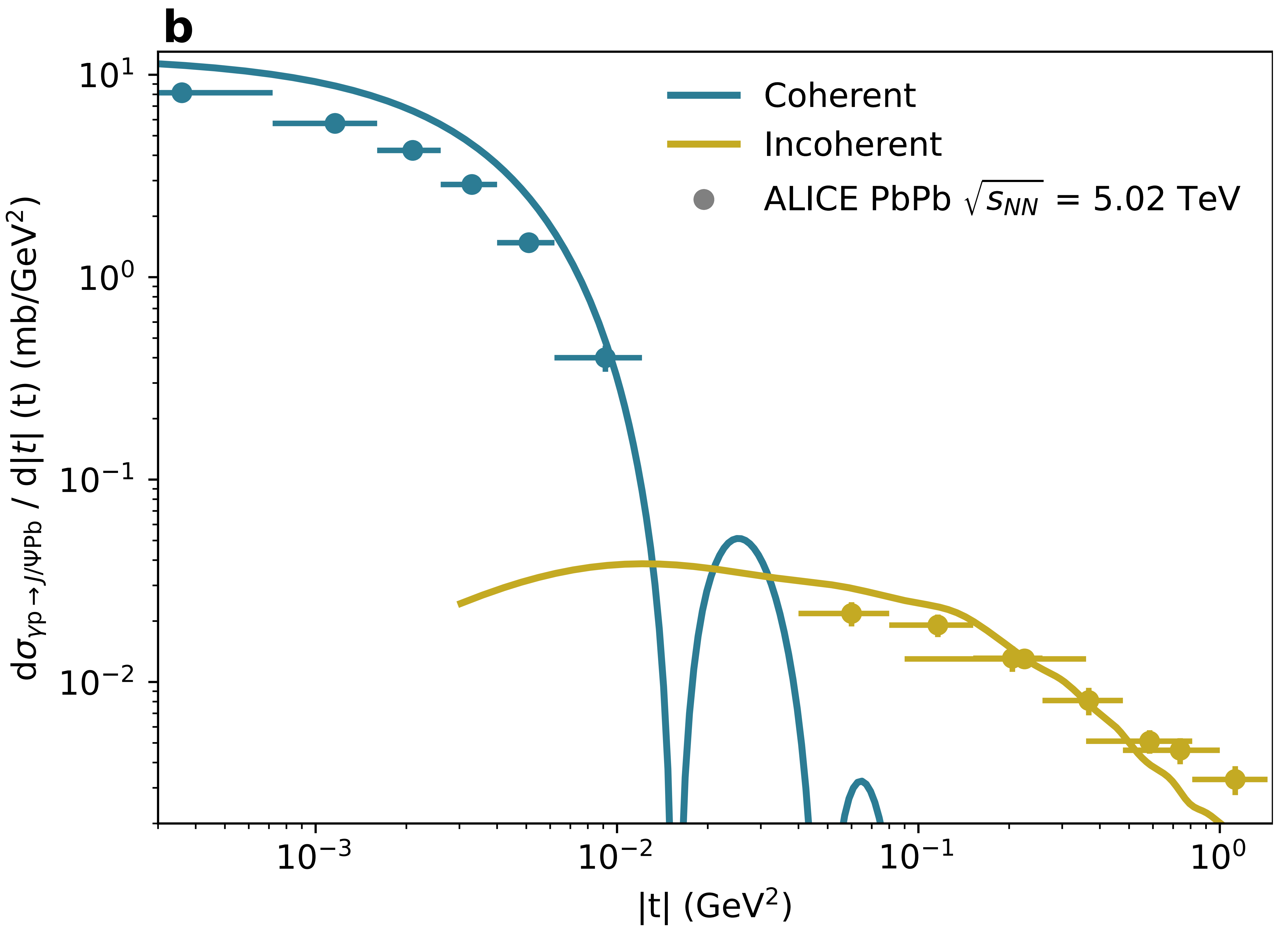

Mandelstam-t dependence of coherent (blue) and incoherent (gold) J/ψ photo-production off Pb.

ENERGY-DEPENDENT HOT–SPOT MODEL

LEAD

$$\frac{\mathrm{d}\sigma^{\mathrm{dip}}_{\mathrm{Pb}}}{\mathrm{d}\vec{b}} = 2\left[1-\left(1-\frac{1}{2A}\sigma_0 N(x,r)T_{\mathrm{Pb}}(\vec{b})\right)^A\right]$$

$$T_{\mathrm{hs}}(\vec{b}-\vec{b}_i) = \frac{1}{2\pi B_{\mathrm{hs}}}\sum_{i=1}^{A=208}\frac{1}{N_{\mathrm{hs}}}\sum_{j=1}^{N_{\mathrm{hs}}}\exp\left(-\frac{\left(\vec{b}-\vec{b}_i-\vec{b}_j\right)^2}{2B_{\mathrm{hs}}}\right)$$

$$N(x,r) = \left[1-\exp\left(-\frac{r^2Q_s^2(x)}{4}\right)\right]$$

$$\langle N_{hs}(x)\rangle = p_0 x^{p_1}(1+p_2\sqrt{x})$$

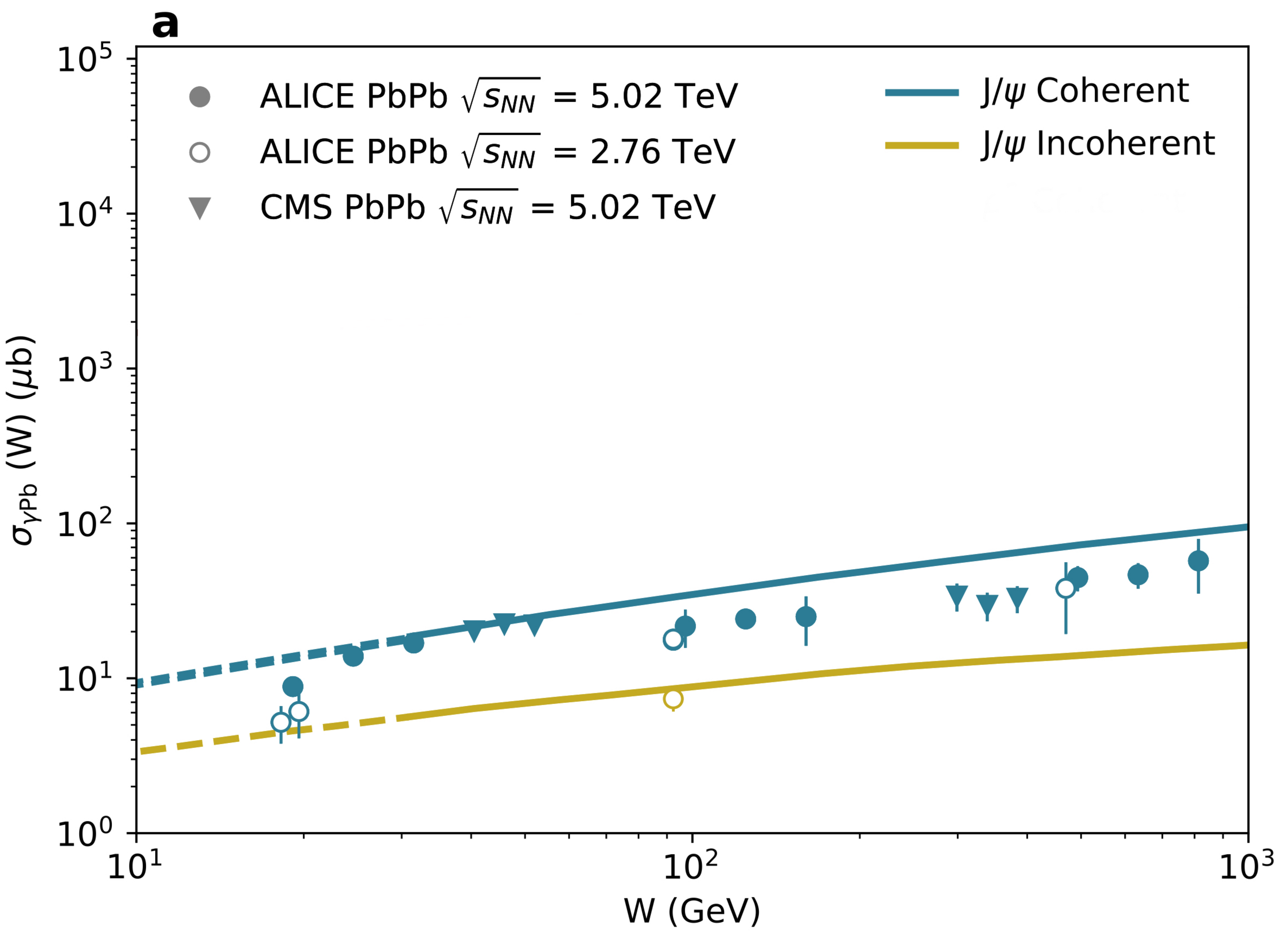

Energy dependence of coherent (blue) and incoherent (gold) J/ψ photo-production off Pb.

ONSET OF GLUON SATURATION

- Incoherent processes are sensitive to two different size scales, that of **NUCLEONS (~ 1 fm)** and that of **HOT SPOTS (~ 0.1 fm)**

- **MANDELSTAM – t** ⟵ FOURIER TRANSFORM ⟶ **MATTER DISTRIBUTION IN THE IMPACT-PARAMETER PLANE**

- scanning the energy behaviour in specific $|t|$ ranges samples fluctuations of different transverse sizes and allows for the isolation of the contribution of hot spots where one expects saturation effects to set in

- lower values of $|t|$ are dominated by the contribution of large size scales

- the cross section at large values of $|t|$ is determined mainly by the variance of objects with a small transverse size

ONSET OF GLUON SATURATION

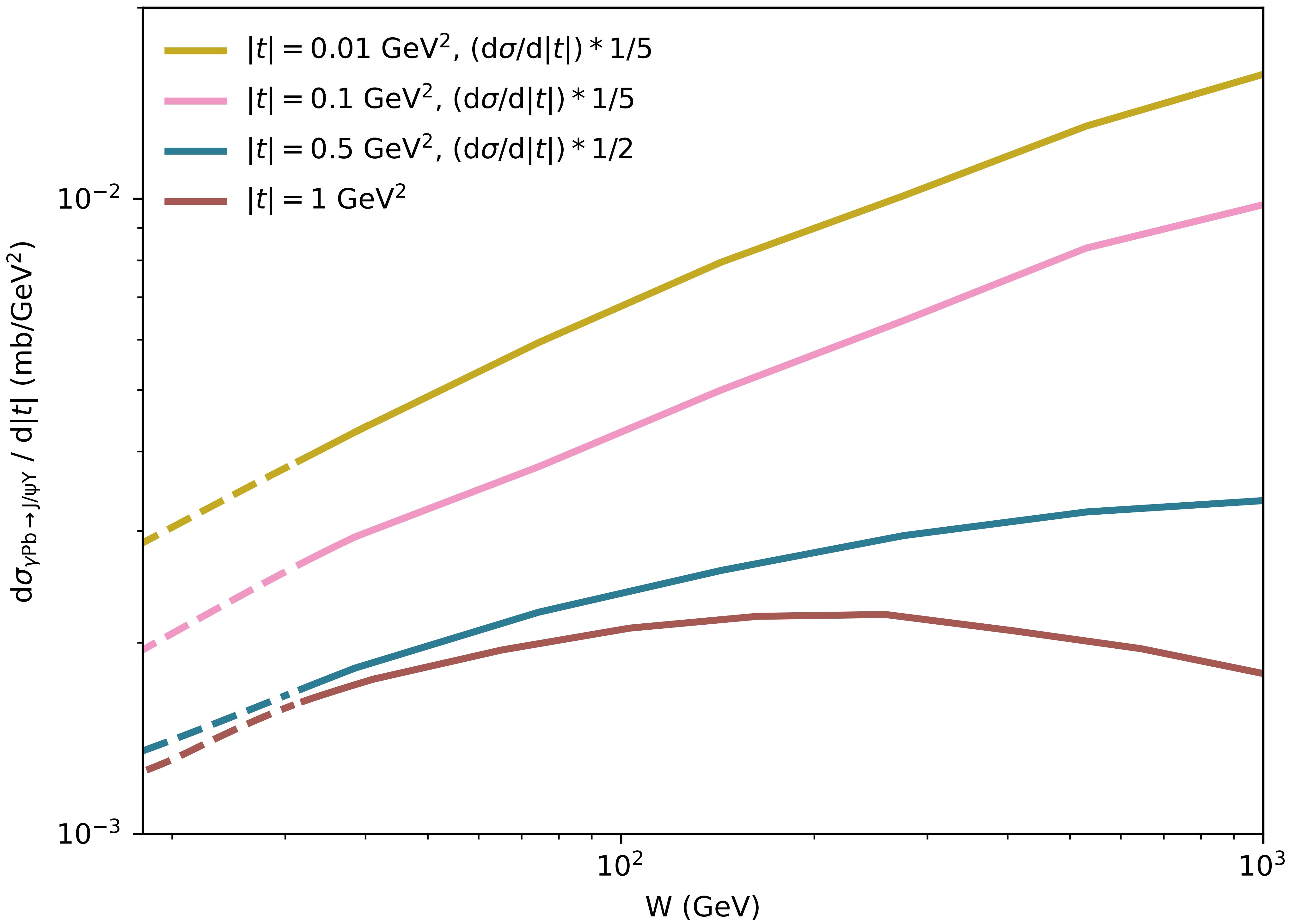

Prediction of the energy-dependent hot-spot model for the incoherent photo-production of J/ψ vector mesons off Pb in diffractive interactions

ONSET OF GLUON SATURATION

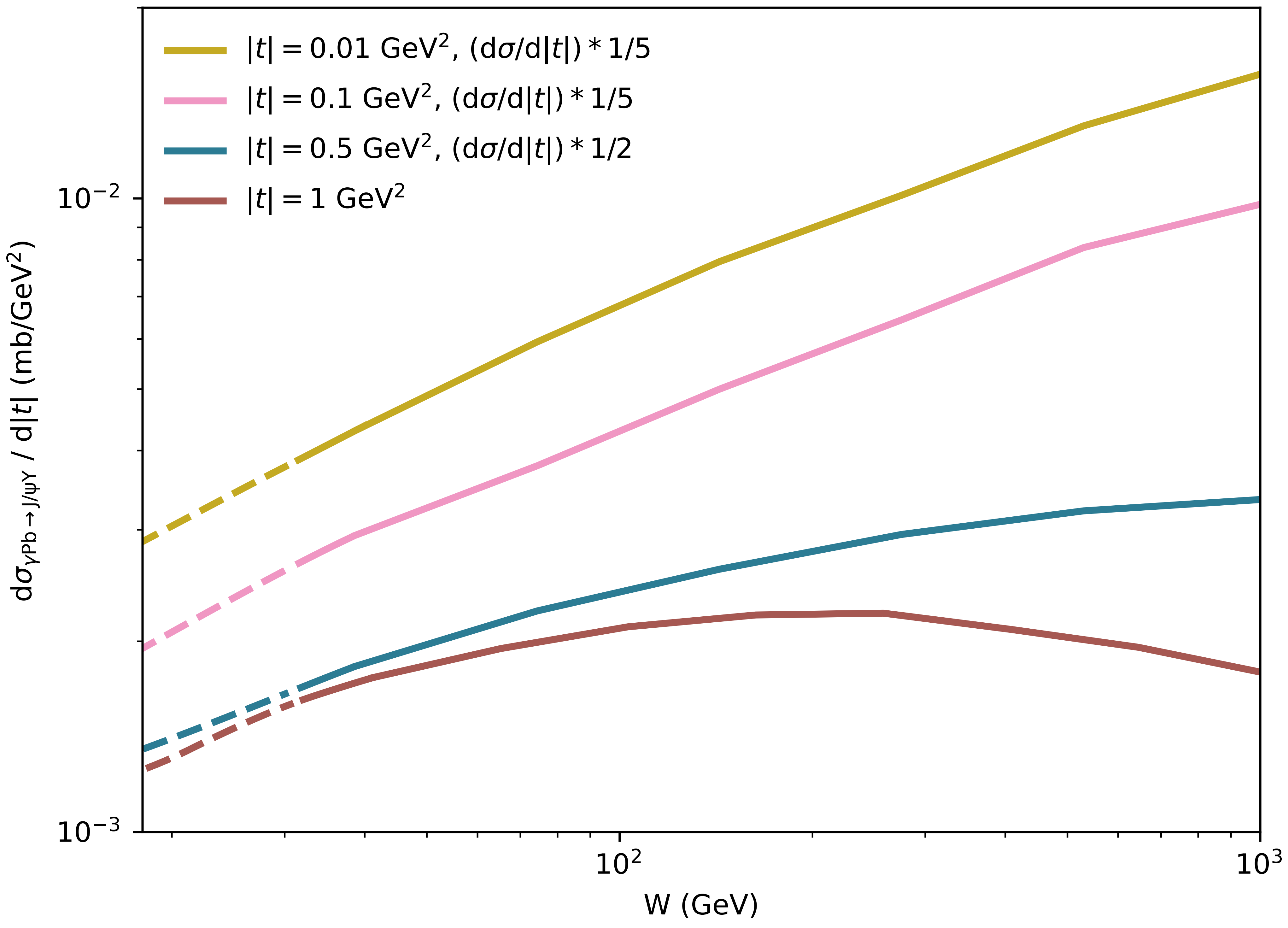

Prediction of the energy-dependent hot-spot model for the incoherent photo-production of J/ψ vector mesons off Pb in diffractive interactions

For small |t| values the cross section raises with energy

ONSET OF GLUON SATURATION

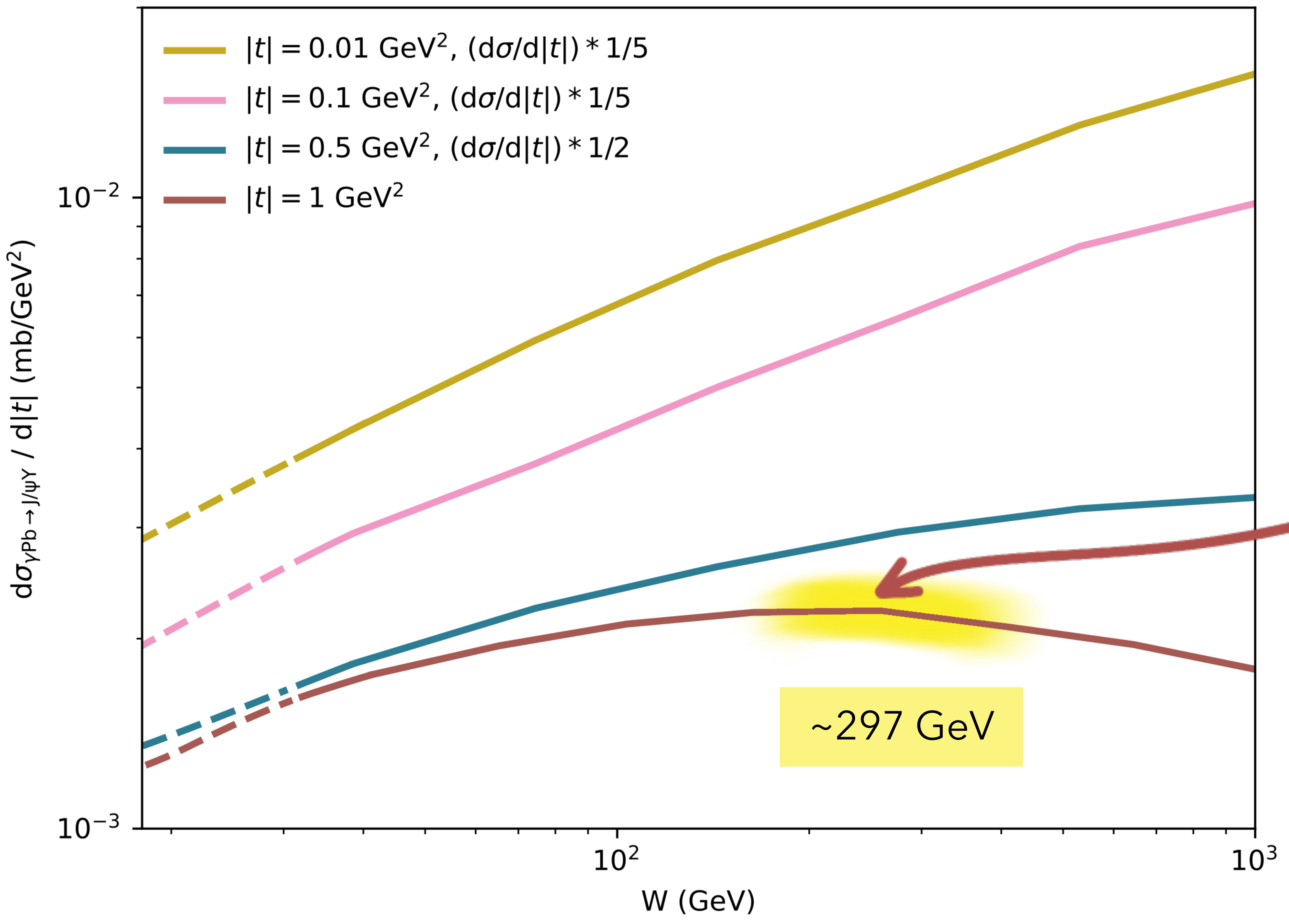

Prediction of the energy-dependent hot-spot model for the incoherent photo-production of J/ψ vector mesons off Pb in diffractive interactions

For small |t| values the cross section raises with energy

At larger values of |t|, the rise of the cross section reaches a maximum and then decreases

ONSET OF GLUON SATURATION

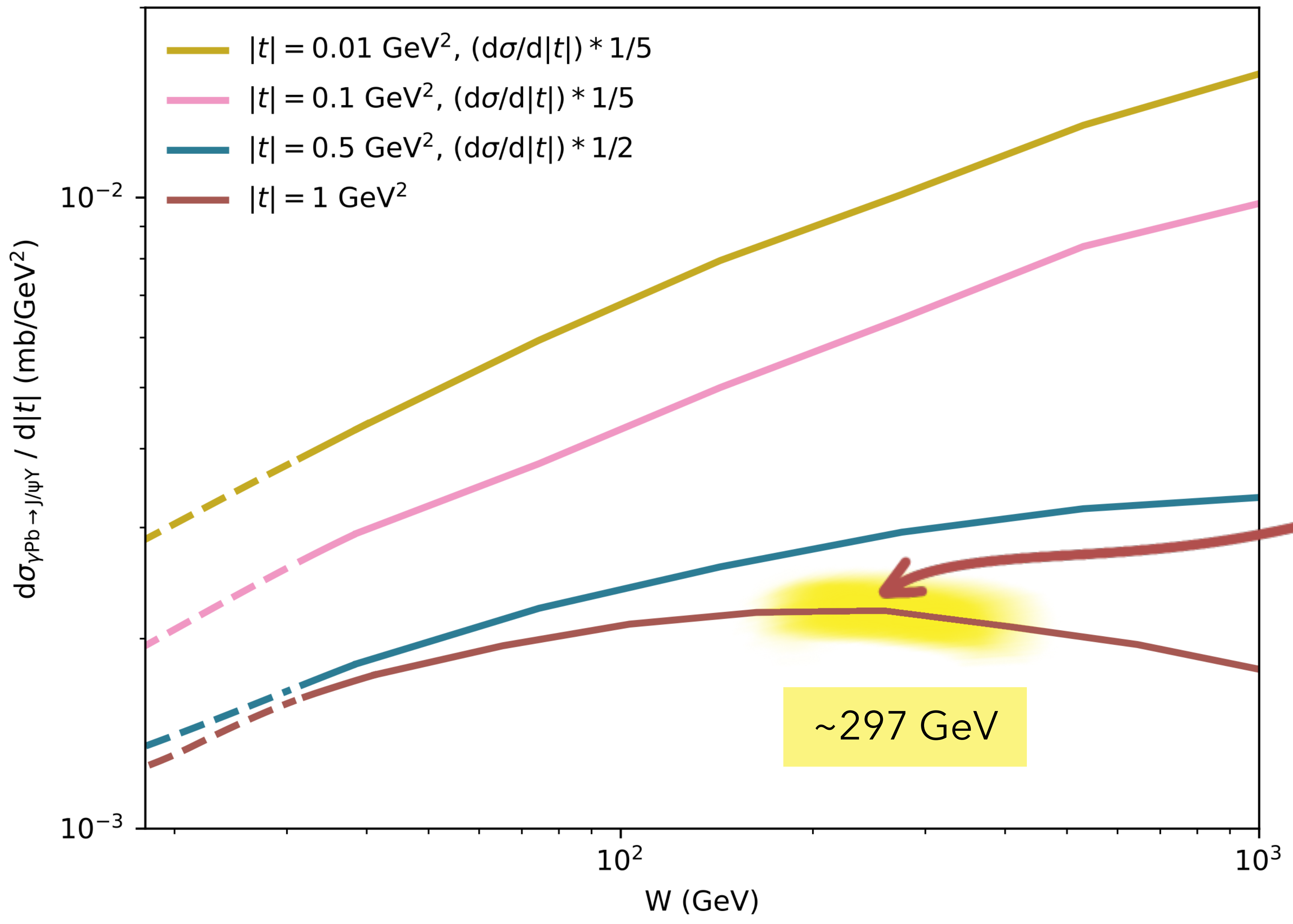

Prediction of the energy-dependent hot-spot model for the incoherent photo-production of J/ψ vector mesons off Pb in diffractive interactions

For small |t| values the cross section raises with energy

At larger values of |t|, the rise of the cross section reaches a maximum and then decreases

- The shape for the W dependence at a fixed value of |t| can be described by $f(W) = N\,(W/W_0)^{\delta} \exp\big(-(W/W_0)(\delta/W_{\max})\big)$
  - Fitting this function to the prediction at |t| = 1 GeV^2 we find $W_{\max}$ to be 297 ± 6 GeV.

ONSET OF GLUON SATURATION

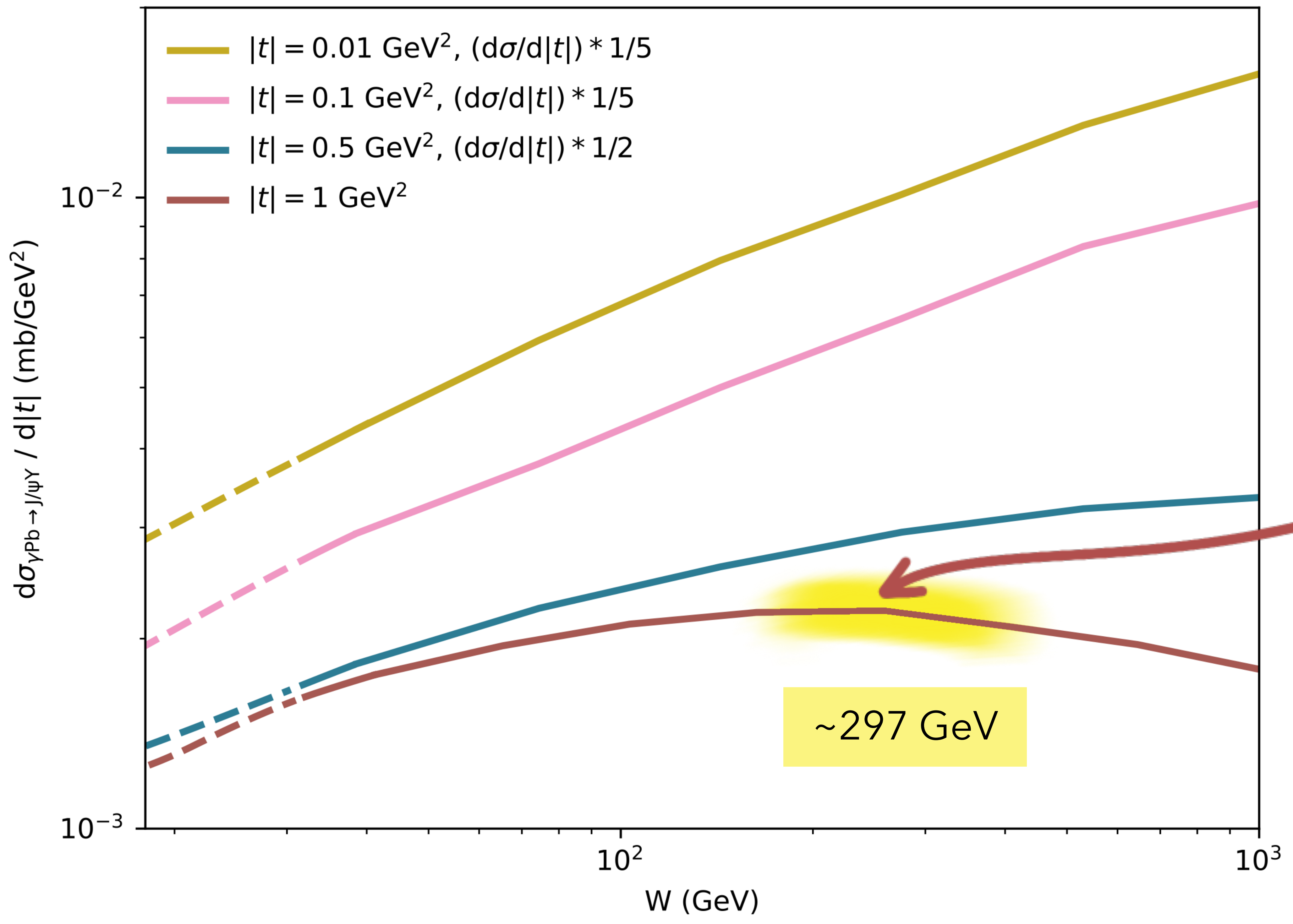

Prediction of the energy-dependent hot-spot model for the incoherent photo-production of J/ψ vector mesons off Pb in diffractive interactions

For small |t| values the cross section raises with energy

At larger values of |t|, the rise of the cross section reaches a maximum and then decreases

- The shape for the W dependence at a fixed value of |t| can be described by $f(W) = N\,(W/W_0)^{\delta}\exp\big(-(W/W_0)(\delta/W_{\max})\big)$
  - Fitting this function to the prediction at |t| = 1 GeV^2 we find $W_{\max}$ to be 297 ± 6 GeV.

THE MAXIMUM MARKS THE ONSET OF SATURATION EFFECTS AND IT IS WELL WITHIN THE REACH OF THE LHC

SUMMARY

PROTON	LEAD

SUMMARY

PROTON

- The model predicts that the energy dependence of the dissociative process increases from low energies up to W ~ 500 GeV and then decreases steeply - this energy range can be explored at LHC.

arXiv:1608.07559 [hep-ph]

LEAD

SUMMARY

PROTON

- The model predicts that the energy dependence of the dissociative process increases from low energies up to W ~ 500 GeV and then decreases steeply - this energy range can be explored at LHC.

arXiv:1608.07559 [hep-ph]

LEAD

- The model predicts that the onset of gluon saturation can be uniquely identified using incoherent J/ψ production in Pb–Pb collisions at currently accessible energies of the LHC.

arXiv:2312.11320 [hep-ph]

SUMMARY

PROTON

- The model predicts that the energy dependence of the dissociative process increases from low energies up to W ~ 500 GeV and then decreases steeply - this energy range can be explored at LHC.

arXiv:1608.07559 [hep-ph]

LEAD

- The model predicts that the onset of gluon saturation can be uniquely identified using incoherent J/ψ production in Pb–Pb collisions at currently accessible energies of the LHC.

THE EXPERIMENTAL OBSERVATION OF SUCH AN EFFECT WOULD ENABLE US TO PINPOINT THE ONSET OF SATURATION AND ADD A PIECE OF STRONG EVIDENCE FOR ITS EXISTENCE

arXiv:2312.11320 [hep-ph]

Phys. Lett. B 852 (2024) 138613

Contents lists available at ScienceDirect

Physics Letters B

journal homepage: www.elsevier.com/locate/physletb

ELSEVIER

Letter

Incoherent J/ψ production at large $|t|$ identifies the onset of saturation at the LHC

J. Cepila, J.G. Contreras, M. Matas *, A. Ridzikova

Faculty of Nuclear Sciences and Physical Engineering, Czech Technical University in Prague, Czech Republic

ARTICLE INFO

Editor: F. Gelis

Keywords:
QCD
Gluon saturation
LHC
Diffraction
Low-x physics

ABSTRACT

We predict that the onset of gluon saturation can be uniquely identified using incoherent J/ψ production in Pb–Pb collisions at currently accessible energies of the LHC. The diffractive incoherent photo-production of a J/ψ vector meson off a hadron provides information on the partonic structure of the hadron. Within the Good-Walker approach it specifically measures the variance over possible target configurations of the hadronic colour field. For this process then, gluon saturation sets in when the cross section reaches a maximum, as a function of the centre-of-mass energy of the photon-hadron system (W), and then decreases. We benchmark the energy-dependent hot-spot model against data from HERA and the LHC and demonstrate a good description of the available data. We show that the study of the energy dependence of the incoherent production of J/ψ allows us to pinpoint the onset of saturation effects by selecting the region of Mandelstam-t around 1 GeV^2 where the contribution of hot spots is dominant. We predict the onset of saturation in a Pb target to occur for W around a few hundred GeV. This can be measured with current data in ultra-peripheral Pb–Pb collisions at the LHC.

BACKUP SLIDES

- The number of hot spots grows with energy and N_{hs} is generated integer value from a zero-truncated Poisson distribution with the mean value

$$\langle N_{hs}(x) \rangle = p_0 x^{p_1} (1 + p_2 \sqrt{x})$$

$$p_0 = 0.015,\ p_1 = -0.58,\ p_2 = 300$$

- The physics explanation according to the parton saturation phenomenon is that the growth of the number of scattering centers provides the growth of the exclusive and dissociative cross section. However, at some point the number of hot spots is so large that they overlap. When the overlap is large enough, different configurations look the same and the variance diminishes and so does the dissociative cross section.

- The physics explanation according to the parton saturation phenomenon is that the growth of the number of scattering centers provides the growth of the exclusive and dissociative cross section. However, at some point the number of hot spots is so large that they overlap. When the overlap is large enough, different configurations look the same and the variance diminishes and so does the dissociative cross section.

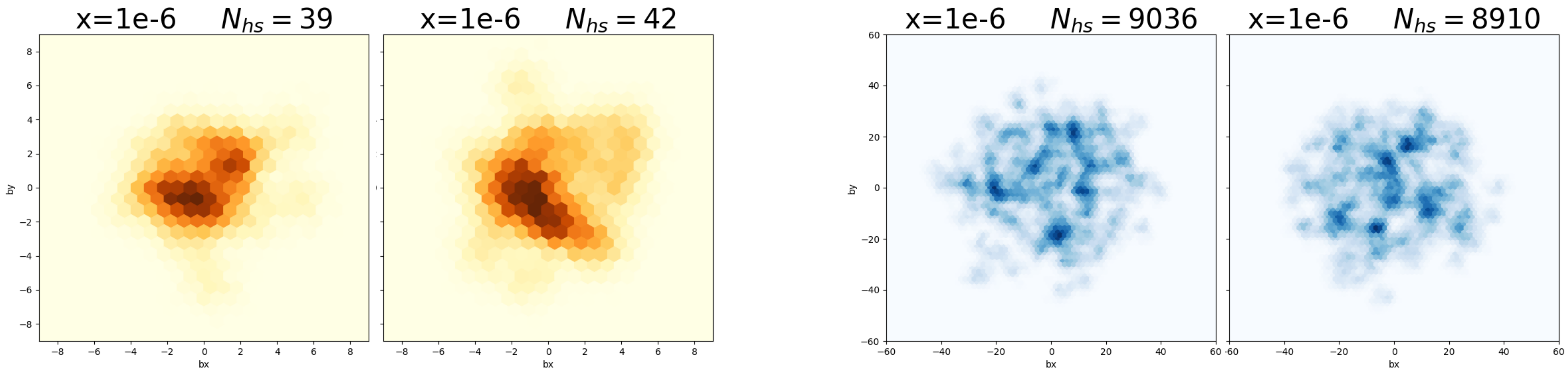

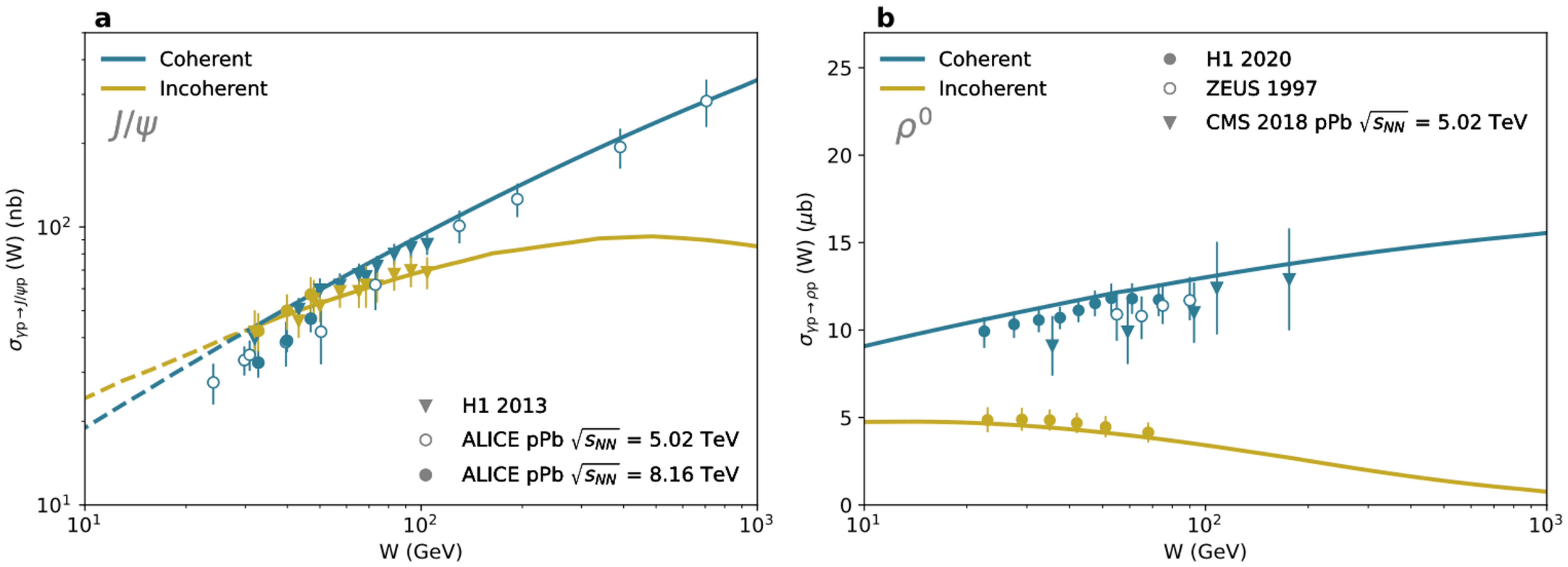

Fig. 1. Diffractive photo-production of J/ψ (**a**) and ρ^0 (**b**) off protons for the coherent (blue) and incoherent (gold) processes. The markers show measured data from the H1 [30,31], ALICE [32–34], and CMS [35] collaborations, while the lines depict the predictions of our model. The dashed line represents values of W that correspond to x greater than 0.01, where the validity of the formalism is questionable.

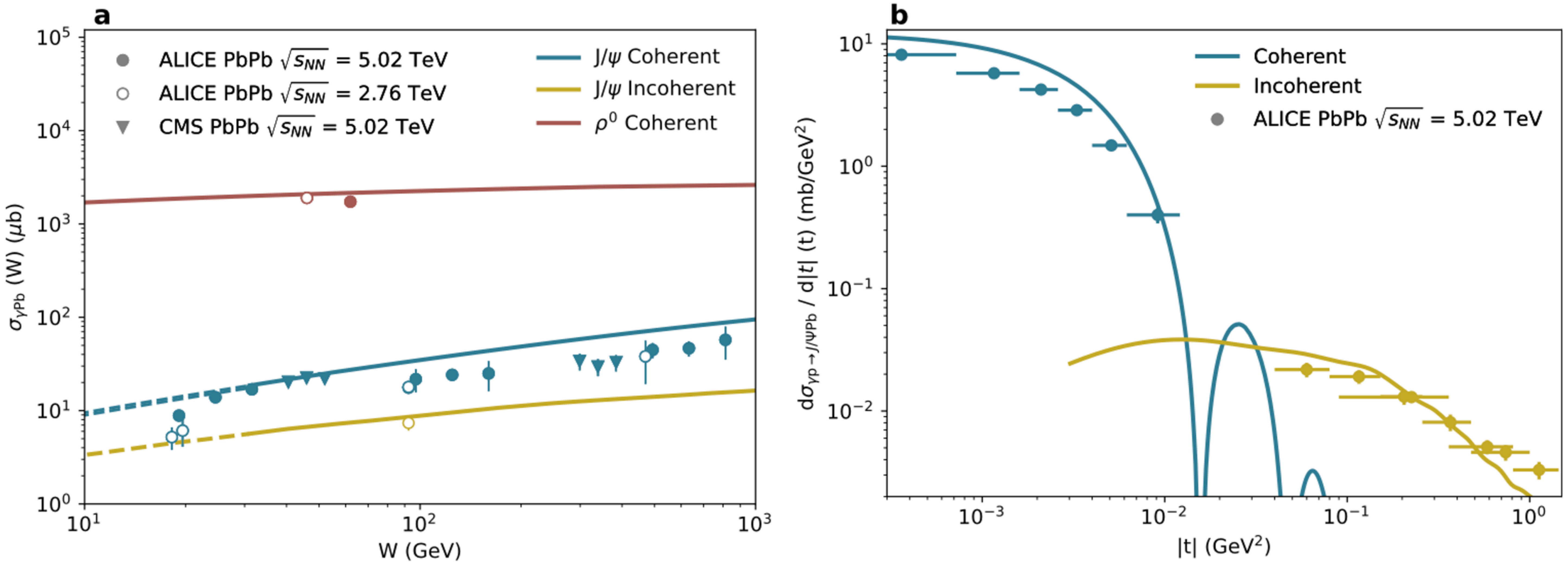

Fig. 2. a: Energy dependence of ρ^0 and J/ψ photo-production off Pb. **b:** Mandelstam-t dependence of coherent (blue) and incoherent (gold) J/ψ photo-production off Pb at an energy $W \approx 125$ GeV. The markers show data from the ALICE [36–40] and CMS [41] collaborations at the LHC, while the lines depict the predictions of our model.